

MOL1107

**SPECIFIC INHIBITION OF NF- κ B-DEPENDENT INFLAMMATORY
RESPONSES BY CELL TYPE-SPECIFIC MECHANISMS UPON A_{2A}
ADENOSINE RECEPTOR GENE TRANSFER**

William A. Sands, Anthony F. Martin, Elaine W. Strong and Timothy M. Palmer

Molecular Pharmacology Group, Division of Biochemistry and Molecular Biology

Institute of Biomedical and Life Sciences, University of Glasgow

Glasgow G12 8QQ, Scotland, U.K.

MOL1107

RUNNING TITLE PAGE

Running Title Anti-inflammatory effects of A_{2A}AR gene transfer

Corresponding author T.M. Palmer, Ph.D., 425 Davidson Bldg., University of Glasgow,
Glasgow, G12 8QQ, U.K. Phone +44 141 330 4626. Fax +44 141 330 4620.

E-mail T.Palmer@bio.gla.ac.uk

Number of pages of text = 25. Number of tables = 0. Number of figures = 12

Number of references = 46. Words in Abstract/Introduction/Discussion = 230/392/1519

Abbreviations

BSA, bovine serum albumin; CGS21680, 2-(*p*-carboxyethyl)phenylamino-5'-*N*-ethylcarboxamidoadenosine; CPA, *N*⁶-cyclopentyladenosine; DMEM, Dulbecco's modified Eagle's medium; EMSA, electrophoretic mobility shift assay; ERK, extracellular signal-regulated kinase; GFP, green fluorescent protein; G-protein, guanine nucleotide-binding regulatory protein; HEK, human embryonic kidney; HRP, horseradish peroxidase; HUVEC, human umbilical vein endothelial cells; iNOS, inducible nitric oxide synthase; JNK, c-jun N-terminal kinase; NECA, 5'-*N*-ethylcarboxamidoadenosine; PBS, phosphate-buffered saline; PDTC, pyrrolidine dithiocarbamate; PBSGG, PBS/goat serum/gelatin; TNF α , tumour necrosis factor α ; ZM241385, 4-(2-[7-amino-2-{2-furyl}{1,2,4}triazolo{2,3-a}{1,3,5}triazin-5-yl-amino]ethyl)phenol

MOL1107

ABSTRACT

Adenosine is a potent inhibitor of inflammatory processes, and the A_{2A} adenosine receptor (A_{2A}AR) plays a key non-redundant role as a suppresser of inflammatory responses *in vivo*. Here we demonstrate that increasing A_{2A}AR gene expression suppressed multiple inflammatory responses in both human umbilical vein endothelial cells (HUVECs) and rat C6 glioma cells *in vitro*. Specifically, the induction of the adhesion molecule E-selectin by either tumour necrosis factor α (TNF α) or *E. coli* lipopolysaccharide (LPS) was reduced by over 70% in HUVECs, while inducible nitric oxide synthase (iNOS) induction was abolished in C6 cells following exposure to interferon- γ in combination with LPS and TNF α , suggesting that the receptor inhibited a common step in the induction of each of these pro-inflammatory genes. Consistent with this hypothesis, A_{2A}AR expression inhibited the activation of NF- κ B, a key transcription factor whose proper function was essential for optimal iNOS and E-selectin induction. However, while NF- κ B binding to target DNA was severely compromised in both cell types, the mechanisms by which this occurred were distinct. In C6 cells, A_{2A}AR expression blocked I κ B α degradation by inhibiting stimulus-induced phosphorylation, while in HUVECs A_{2A}AR expression inhibited NF- κ B translocation to the nucleus independently of any effect on I κ B α degradation. Together, these observations suggest that A_{2A}AR-mediated inhibition NF- κ B activation is a critical aspect of its anti-inflammatory signalling properties, and that the molecular basis of this inhibition varies in a cell type-specific manner.

MOL1107

INTRODUCTION

Extracellular levels of the ubiquitous nucleoside adenosine are a critical regulator of cardiovascular and central nervous system homeostasis. Upon its extracellular accumulation following metabolic stress, adenosine exerts a plethora of protective effects on target tissues that are mediated by its binding to four types of cell surface G-protein-coupled adenosine receptor (AR) proteins, termed A₁, A_{2A}, A_{2B} and A₃ (Fredholm *et al.*, 2001; Linden, 2001). Importantly, several inflammatory cell types have been shown to be particularly responsive to the adenosine released during hypoxia, including neutrophils, endothelial cells (ECs) and glial cells (Banerjee *et al.*, 2002; Sitkovsky *et al.*, 2004). From these studies, the A_{2A}AR signalling system has emerged as a key pathway by which excessive inflammatory responses can be attenuated. For example, phorbol ester-mediated increases in neutrophil adhesion to ECs isolated from porcine aorta can be inhibited by prior treatment of ECs with A_{2A}AR agonists NECA and CGS21680 but not by the A₁AR-selective agonist N⁶-cyclopentyladenosine (CPA) (Felsch *et al.*, 1995). Secondly, exposure of human umbilical vein ECs (HUVECs) to exogenous adenosine partially reduces TNF α -stimulated leukocyte adhesion by inhibiting the induction of VCAM-1 and E-selectin, two critical adhesion molecules that mediate EC-leukocyte interaction, and also by inhibiting the induction of at least two pro-inflammatory cytokines, interleukin (IL)-1 and IL-6 (Bouma *et al.*, 1996). Thirdly, the non-steroidal anti-inflammatory drugs sulfasalazine and methotrexate exert their anti-inflammatory effects by promoting ecto-5'-nucleotidase-mediated conversion of adenine nucleotides to adenosine. The resulting elevated levels of adenosine can then act upon endogenous A_{2A} and A₃ARs on ECs and neutrophils to inhibit inflammatory responses (Cronstein *et al.*, 1999; Montesinos *et al.*, 2000). Finally, the importance of the A_{2A}AR as a constitutive repressor of inflammatory responses *in vivo* has

MOL1107

been demonstrated by the enhanced responses to bacterial endotoxin observed in mice in which the $A_{2A}AR$ gene has been deleted (Ohta and Sitkovsky, 2001).

However, despite numerous observations describing the anti-inflammatory effects of $A_{2A}AR$ activation in a variety of cellular systems, relatively little is known about the molecular mechanisms by which they occur. In this study, we demonstrate that elevating $A_{2A}AR$ protein expression in glioma cells and vascular ECs is sufficient to markedly inhibit inflammatory responses to maximally effective concentrations of pro-inflammatory stimuli. In addition, we demonstrate that the receptor can exert these effects by specifically blocking activation of the critical transcription factor NF- κ B *via* distinct cell type-specific mechanisms.

MATERIALS AND METHODS

Materials The human A_{2A}AR gene was generously donated by Dr. Andrea Townsend-Nicholson (Royal Free Hospital, London, U.K.). GeneJuice transfection reagent was from Novagen. HUVECs plus appropriate growth medium and supplements were from Cambrex. Nucleofection reagents were from Amaxa. Antibodies were obtained from Santa Cruz Biotechnology (I κ B α [sc371], RelA/p65[sc109], 12CA5[sc7392]), Serotec (E-selectin monoclonal antibody 1.2B6), BD Biosciences (inducible nitric oxide synthase (iNOS)) and Cell Signalling Technology (Ser³²Ser³⁶-phosphorylated I κ B α , Ser⁶³-phosphorylated c-jun, Thr¹⁸⁰Tyr¹⁸²-phosphorylated and total p38). The NF- κ B oligonucleotide probe was from Santa Cruz. *E. Coli* 0111:B4 LPS, rat and human TNF α and rat interferon- γ (IFN γ) were from Sigma-Aldrich. A 3- κ B enhancer conA-luciferase reporter plasmid as well as sheep non-immune, anti-p50 and p65 antibodies used for supershift experiments were generously donated by Prof. Ron Hay (University of St. Andrews, U.K.). A control pSV- β -galactosidase expression construct was from Promega. A bacterial expression plasmid that directed expression of GST-c-jun(1-79) and rabbit anti-JNK1,2 polyclonal antibody were generously donated by Prof. David Gillespie (Cancer Research U.K. Beatson Laboratories, Glasgow, U.K.). A control adenovirus (AV) that directed the expression of GFP alone, termed AV/GFP, was generously donated by Prof. Miles Houslay (University of Glasgow, U.K.). pcDNA3/HA-tagged wild type (WT) I κ B α was generously donated by Prof. Warner Greene (Gladstone Institute of Virology and Immunology, University of California, San Francisco, CA). Sources of other materials have been described elsewhere (Palmer and Stiles, 1999).

Cell culture HUVECs were propagated in ECM-2 medium supplemented with 2% (w/v) fetal bovine serum, hydrocortisone, ascorbate and recombinant growth factors as recommended by the supplier (Cambrex). Human embryonic kidney 293 (HEK293) and C6

MOL1107

glioma cells were propagated in Dulbecco's modified Eagle's medium (DMEM) supplemented with 10% (v/v) fetal bovine serum, 1 mM L-glutamine, 100 units/ml penicillin and 100 µg/ml streptomycin. The generation and characterisation of the C6 cell lines used in this study have been described elsewhere (Palmer and Stiles, 1999). All cells were grown at 37°C in a humidified atmosphere containing 5% (v/v) CO₂.

Generation of a myc epitope-tagged human A_{2A}AR Myc epitope (EQKLISEEDL) and His₆ sequences were added to the carboxyl-terminus of the human A_{2A}AR by PCR using pCMV5/human A_{2A}AR cDNA as the template. The primers were 5'-TAGCAGAGCTCGTTTAGT-3', which anneals within pCMV5 upstream of the A_{2A}AR initiating Met, and 5'-TGATTTCTAGAGGACACTCCTGCTCCATCCTG-3', which was designed to remove the A_{2A}AR stop codon and add a *Xba*I site (in bold). This was to allow in-frame fusion of the A_{2A}AR upstream of the myc epitope and His₆ sequences in pcDNA3/mycHisA (Invitrogen) following ligation of *Hind*III/*Xba*I-digested vector and similarly digested PCR product. The integrity of the generated open reading frame was verified by DNA sequencing.

Generation of recombinant serotype 5 AV encoding myc-humA_{2A}AR The myc-humA_{2A}AR open reading frame was excised from pcDNA3/mycHisA by *Hind*III/*Pme*I digestion and subcloned into *Hind*III/*Eco*RV-digested shuttle vector pAdTrackCMV: the subcloning procedure destroyed the *Eco*RV and *Pme*I sites. The resulting pAdTrackCMV/myc-humA_{2A}AR construct was then linearised at the remaining *Pme*I site within the vector to expose the inverted terminal repeats, and co-transformed with pAdEasy1 into *E. coli* strain BJ5183 by electroporation in 2.0 mm cuvettes at 2500V, 200Ω, and 25 µF. Successful pAdEasy1/myc-humA_{2A}AR recombinants were identified by *Pme*I digestion and PCR using myc-humA_{2A}AR-specific primers, and expanded in *E. coli* XL1 Blue. Plasmid DNA prepared from chosen clones was then digested with *Pac*I and transfected using

MOL1107

Lipofectamine into low-passage HEK293 cells to initiate viral production. Large-scale amplification and titration of AV/GFP and AV/myc-humA_{2A}AR viral stocks were performed as described by He *et al.* (1998).

For infection, HUVECs were washed in regular growth medium and then incubated overnight with the same medium supplemented with recombinant AV at the m.o.i.'s indicated in the Results and Figure Legends. The next day, the virus-containing medium was aspirated and replaced with normal medium. Cells were used for analysis twenty four hours later.

Luciferase assays of reporter gene transcription in C6 glioma cells C6 cells at 70-80% confluence in six-well dishes were transfected with 1 µg/well each of 3-κB enhancer conA-luciferase and pSVβ-galactosidase plasmids using 7 µl of GeneJuice according to the manufacturer's instruction. Forty eight hours later, cells were treated as described in the Figure Legends. Reactions were terminated by placing on ice and washing twice with ice-cold PBS prior to harvesting by scraping into 50 µl lysis buffer (50 mM potassium phosphate, pH 7.8, 0.2% (v/v) Triton X-100 and 0.5 mM DTT) which was clarified by centrifugation at 48,000g for 15 min. 15 µl of the supernatant was used for determination of β-galactosidase activity according to manufacturer's instructions. 25 µl was added to luciferase assay buffer (50 mM Tris phosphate, pH 7.8, 16 mM magnesium chloride, 2 mM DTT 1.8% (v/v) Triton X-100 and 30% (v/v) glycerol) for determination of luciferase activity in a 96-well luminometer plate. Samples were assayed in triplicate and luciferase activity normalised to β-galactosidase activity.

Transient transfection of HUVECs Endotoxin-free cDNA expression constructs were prepared using the Wizard Purefection plasmid DNA purification system (Promega). These were introduced into HUVECs using the Amaxa nucleofection kit, as per manufacturer's instructions. Briefly, 1x10⁶ HUVECs per sample were resuspended in 100 µl of

MOL1107

nucleofection buffer containing 1 μg of pMaxGFP (to assess transfection efficiency) and 4 μg of either pcDNA3 (vector control) or pcDNA3/HA-tagged WT I κ B α . Plasmid DNA was introduced into the nucleus of the cells using an Amaxa NucleofectorTM set at program U-01. Cells were then seeded into 96-well plates and E-selectin induction assessed 48 hrs later by ELISA.

¹²⁵I-ZM241385 synthesis and saturation binding ¹²⁵I-ZM241385 was synthesised, purified by HPLC and utilised in radioligand binding studies on freshly isolated HUVEC membranes as described by Palmer *et al.* (1995).

Monocyte adhesion assay 1×10^4 HUVECs/well were seeded into a 24-well plate and grown overnight. The cells were then infected for 24 hours at a m.o.i. of 25 pfu/cell with recombinant AVs. Following treatment as indicated in the Figure Legends, the medium was aspirated and HUVEC monolayers overlaid with 1×10^5 U937 promonocytic cells/well. The cells were allowed to adhere for 1 hr at 37°C prior to removal of the medium and washing of monolayers three times with 1 ml/well serum-free DMEM to remove any non-adherent U937 cells. The cells were then fixed in 0.5 ml/well 4% (w/v) paraformaldehyde in 5% (w/v) sucrose/PBS, pH 7.2, and analysed using a combination of fluorescence and brightfield microscopy to determine the number of U937 cells adhering to GFP-expressing HUVECs. At least 300 GFP-expressing cells were counted in 3-5 separate fields to calculate the average number of adherent cells per 100 GFP-expressing HUVECs for any given treatment.

ELISA for cell surface E-selectin expression 1×10^5 HUVECs/well were seeded in a 96-well plate and grown to 70% confluence. The cells were then infected for 24 hours at a m.o.i. of 25 pfu/cell with recombinant AVs. The following day, cells were treated with TNF α for the time period indicated in the Figure Legends. The incubation was stopped by transferring the plate to ice and cells were washed gently three times with 0.2 ml/well ice-cold PBS. Cells

MOL1107

were then fixed by overnight incubation at 4°C with 0.1 ml/well 4% (w/v) paraformaldehyde in 5% (w/v) sucrose/PBS, pH 7.2. The next day, each well was washed gently three times with PBS and then incubated for 1 hr at room temperature in PBS containing 0.1% (w/v) BSA to block non-specific antibody binding sites. Following three more washes with PBS, 0.1 ml anti-E-selectin antibody diluted 1:1000 in PBS/0.1% (w/v) BSA was added to each well. A parallel set of isotype control incubations using anti-hemagglutinin antibody 12CA5 at 1:1000 dilution was included to assess non-specific antibody binding. Following a 2 hr incubation at room temperature, antibody solution was removed and the cells washed three times with PBS before the addition of 0.1 ml/well horseradish peroxidase (HRP)-conjugated anti-mouse IgG diluted 1:1000 in PBS/0.1% (w/v) BSA and incubation for 1 hr at room temperature. Wells were then washed five times with PBS before the addition of 0.1 ml/well 3,3',5,5'-tetramethylbenzidine. The reaction was allowed to develop at room temperature prior to A₆₀₀ determination using a plate reader.

Griess assay of nitrite accumulation Confluent C6 cells in 6-well plates were incubated in normal medium with the stimuli indicated in the Figure Legends. Synthesis of nitric oxide was determined by assay of culture supernatants for nitrite, a reaction product of nitric oxide and molecular oxygen. Briefly, 0.2 ml of culture supernatant was allowed to react with 0.2 ml of Griess reagent (Hevel and Marletta, 1994) and incubated at room temperature for 15 min. Following transfer to a 96-well plate, sample absorbance at 570 nm was determined using a plate reader. Fresh culture media served as the blank in all experiments, and nitrite concentrations from experimental samples were calculated from a standard curve derived from the parallel reaction of known amounts of sodium nitrite.

Immunoblotting Confluent HUVECs or C6 cells in six-well plates were treated as described in the Figure Legends prior to washing in ice-cold PBS and solubilisation by scraping into 0.2 ml/well electrophoresis sample buffer (50 mM Tris-HCl, pH 6.8, 10% (v/v) glycerol, 2%

MOL1107

(w/v) SDS) at room temperature. Following brief probe sonication, insoluble material was pelleted by microcentrifugation and the supernatant assayed for protein content using a bicinchonic acid assay. Samples equalised for protein content (typically 50-70 µg/sample) were fractionated by SDS-PAGE on 10 or 12% (w/v) resolving gels. Following transfer to nitrocellulose, membranes were blocked for one hour at room temperature in blocking solution (5% (w/v) skimmed milk in PBS containing 0.1% (v/v) Tween-20). Membranes were then incubated overnight at 4°C with primary antibody diluted in fresh blocking buffer. Primary antibodies were each used at a final concentration of 1 µg/ml. Following three washes in blocking solution, membranes were incubated for one hour at room temperature with appropriate HRP-conjugated secondary antibody at a 1 in 1000 dilution. After further washes with blocking buffer and PBS, immunoreactive proteins were visualised by enhanced chemiluminescence. For phospho-specific antibodies, a similar protocol was used except that the primary antibodies were diluted in Tris-buffered saline (TBS) containing 1% (w/v) BSA and 0.1% (v/v) Tween-20, and all washes were with TBS/0.1% (v/v) Tween-20. Quantitation was by densitometric scanning of exposed films using Totallab imaging software (Phoretix).

Pull-down assay of c-Jun N-terminal kinase (JNK) activation Confluent C6 cells in 6-well dishes were treated as indicated in the Figure Legends. Incubations were terminated by placing the cells on ice and washing in ice-cold PBS. All subsequent procedures were performed at 4°C unless indicated otherwise. Cells were solubilised in 0.3 ml/well JNK lysis buffer (25 mM Hepes, pH 7.7, 20 mM β-glycerophosphate, 0.3 M sodium chloride, 1.5 mM magnesium chloride, 10 mM sodium fluoride, 0.1 mM sodium vanadate, 0.1 mM PMSF and 10 µg/ml each of soybean trypsin inhibitor and benzamidine). Following isolation of soluble fractions by microcentrifugation, samples equalised for protein content and volume were incubated overnight with rotation with 10 µg recombinant GST-c-jun(1-

MOL1107

79) immobilised to glutathione-Sepharose beads following induction and purification from transformed *E coli* BL21 cultures. Complexes were isolated by brief microcentrifugation, washed three times with wash buffer (20 mM Hepes, 50 mM sodium chloride, 2.5 mM magnesium chloride, 0.1 mM EDTA and 0.05 % (v/v) Triton X-100) and then resuspended in 30 μ l kinase assay buffer (25 mM Hepes, pH 7.5, 10 mM magnesium chloride, 20 mM β -glycerophosphate, 75 mM sodium vanadate) supplemented with 100 μ M ATP and 2 mM DTT. Immobilised JNK was activated by incubation at 30°C for 30 min. Reactions were stopped by the addition of 10 μ l 4X-concentrated electrophoresis sample buffer containing 12% SDS and heating to 95°C for 5 min. Samples were fractionated by SDS-PAGE on 12% (w/v) polyacrylamide resolving gels and transferred to nitrocellulose for immunoblotting with anti-Ser⁶³-phosphorylated c-jun antibody for visualisation of GST-c-Jun(1-79) phosphorylation. Protein-equalised samples from each treatment were also processed in parallel for immunoblotting with anti-JNK1,2 antibody.

Electrophoretic mobility shift assay (EMSA) Following treatment as described in the Figure Legends, confluent 10 cm dishes of HUVEC or C6 cells were washed three times with ice-cold PBS prior to scraping. Cells were pelleted by centrifugation at 400g and lysed by the addition of 0.4 ml/tube Buffer A (10 mM Hepes, pH 7.9, 10 mM potassium chloride, 0.1 mM EDTA, 0.1 mM EGTA, 1mM DTT, 0.625% (v/v) NP-40, 0.5 mM PMSF and 10 μ g/ml each of soybean trypsin inhibitor and benzamidine). The samples were then centrifuged at 48,000g for 30 sec at 4°C, and the supernatant removed. The pellet was resuspended in 50 μ l of buffer B (20 mM Hepes, pH 7.9, 0.45 M sodium chloride, 1mM EDTA, 1mM EGTA, 1mM DTT, 0.5 mM PMSF and 10 μ g/ml each of soybean trypsin inhibitor and benzamidine). Samples were agitated for 15 min at 4°C, centrifuged at 48,000g for 5 min and the protein content of the supernatant determined using a Bradford assay. 5 μ l samples from each nuclear extract were then added to a ³²P-labelled double stranded DNA probe

MOL1107

(10,000 cpm/sample) containing the consensus κ B binding sequence GGGGACTTTC to give a final reaction volume of 25 μ l containing 10 mM sodium Hepes, pH 7.9, 0.1 mM magnesium chloride, 0.1 mM EDTA, 0.5 mM DTT, 10% (v/v) glycerol, 50 mM sodium chloride and 0.625 μ g/ml poly dIdC. Following a 30 min incubation at room temperature, samples were analysed by fractionation on a non-denaturing 6% (w/v) polyacrylamide gel containing 0.5xTBE buffer (45 mM Tris-borate, 1 mM EDTA) followed by autoradiography. For supershift analysis, 1 μ l/sample of sheep polyclonal anti-p65, anti-p50 antibodies or non-immune serum controls were added following the initial binding of the probe, and samples incubated for a further 30 min at room temperature prior to electrophoresis.

Laser-scanning confocal microscopy 1×10^5 HUVECs were plated onto glass coverslips in 6-well plates and cultured overnight. The next day, cells were treated as outlined in the Figure Legends, permeabilised by the addition of 0.4% (v/v) Triton X-100 in PBS for 3 min, then washed with PBS supplemented with 0.1% (v/v) goat serum and 0.2% (w/v) gelatin (PBSGG). Coverslips were then incubated with a 1 in 200 dilution of RelA/p65 antibody. After washing with three changes each of PBSGG and PBS, coverslips were incubated with at room temperature for one hour in a 1 in 200 dilution of Alexa594-conjugated goat anti-rabbit IgG. Following sequential washing with PBSGG and PBS as described above, coverslips were mounted onto glass slides using 40 % (v/v) glycerol in PBS for dual-label confocal microscopy using a Zeiss AxioVERT 100 confocal microscope. Images were collected using dual excitation (488 and 543 nm) and emission (515-540 nm for GFP, and 590-610 nm for Alexa594) filter sets. Single labelled controls ensured that there was no inter-channel bleed-through under these conditions. All collected images were analysed using Metamorph software (Universal Imaging).

MOL1107

Statistical analysis Data are presented in the text as means \pm standard error for the number of experiments indicated, while representative experiments are presented in the figures. Statistical significance was assessed using Student's *t*-test or ANOVA with a α probability of 0.05.

MOL1107

RESULTS

Effect of A_{2A}AR expression on iNOS induction in C6 glioma cells Glial cell inflammation plays an important role in the pathophysiology of Parkinson's and Alzheimer's diseases (Monsonego and Weiner, 2003; Hirsch *et al.*, 2003). To determine the ability of the A_{2A}AR to regulate inflammatory responses in this cell type, rat C6 glioma cells stably expressing the canine A_{2A}AR to a range between 2 and 3 pmol/mg, as determined by saturation binding with the A_{2A}AR-selective antagonist radioligand ¹²⁵I-ZM241385, were utilised (Palmer and Stiles, 1999). The accumulation of nitrite and the associated induction of iNOS were used as inflammatory markers in this system, as iNOS-derived nitric oxide release contributes to the ability of activated glial cells to promote neuronal cell death (Brown and Bal-Price, 2003). While no significant nitrite accumulation was observed when they were added individually, maximally effective concentrations of LPS, TNF α or a combination of the two with IFN γ produced a marked induction of nitrite accumulation in control C6 cells which was abolished in A_{2A}AR-expressing C6 cells (nitrite accumulation in response to LPS/TNF α /IFN γ treatment for 24 hr was reduced by 95 \pm 9% in C6/A_{2A}AR cells *versus* control C6 cells, n=10, *p*<0.05, Figure 1A). This was associated with an abolition of iNOS induction in response to LPS/TNF α /IFN γ even in the absence of the AR agonist NECA (Figure 1B). The constitutive inhibition of iNOS induction observed is unlikely to be due to the accumulation of extracellular adenosine acting on the recombinant receptor for two reasons. Firstly, all cellular incubations presented in this study were performed in the presence of 3 units/ml adenosine deaminase to convert any released adenosine to inosine, which is inactive at the A_{2A}AR (Jin *et al.*, 1997). Secondly, inhibition of iNOS induction could not be reversed significantly by inclusion of the A_{2A}AR-selective antagonist ZM241385 at a concentration that blocks specific binding to the A_{2A}AR (LPS/TNF α /IFN γ

MOL1107

treatment produced a $12\pm 12\%$ increase in nitrite accumulation in vehicle pre-treated C6/A_{2A}AR cells *versus* $5\pm 15\%$ in 1 μ M ZM241385-pretreated cells, $n=3$ $p>0.05$ NS, Figure 1C). Therefore, it is possible that constitutive agonist-independent signalling from the A_{2A}AR is sufficient to block iNOS induction in C6 cells.

The A_{2A}AR acts intracellularly to inhibit iNOS induction Theoretically, it was possible that A_{2A}AR expression was leading to constitutive induction and secretion of anti-inflammatory cytokines or other signalling molecules that were acting extracellularly to inhibit iNOS induction. However, medium taken from A_{2A}AR-expressing C6 cells failed to inhibit LPS/TNF α /IFN γ induction of iNOS expression in control C6 cells (Figure 2). In fact, medium from A_{2A}AR-expressing C6 cells actually potentiated iNOS induction by $62\pm 18\%$ ($p<0.05$, $n=4$) compared with medium from control C6 cells (Figure 2). Therefore, the A_{2A}AR must be acting intracellularly to block the signalling pathways leading to iNOS induction.

Effect of A_{2A}AR expression on the activation of the NF- κ B, JNK and p38 pathways Three key inflammatory signalling pathways activated in response to LPS and TNF α include the NF- κ B pathway and the JNK and p38 stress-activated protein kinase signalling pathways (Manning and Davis, 2003; Kumar *et al.*, 2003; Karin *et al.*, 2004). Immunoblotting of extracts from TNF α -treated control and A_{2A}AR-expressing C6 cells with an antibody *versus* active phosphorylated p38 demonstrated that in both cell types, TNF α produced a transient activation of this kinase which peaked by 5 min and had returned to basal by 30 min (Figure 3A). Expression of the A_{2A}AR produced a $25\pm 6\%$ ($p<0.05$, $n=3$) decrease in the maximal extent to which p38 was activated after normalisation to total p38 expression. *In vitro* kinase assays of JNK activation demonstrated that A_{2A}AR expression had no significant effect on either the maximal extent of TNF α stimulation (maximal activation reduced by $9\pm 6\%$ at 15 min, $p>0.05$ NS, $n=3$; Figure 3B) or total JNK expression levels (Figure 3B).

MOL1107

Consistent with a minimal effect on JNK activation, TNF α stimulation of AP-1 activity, as determined following transient transfection of an AP1-luciferase reporter construct, was also not significantly different between control and A_{2A}AR-expressing C6 cells (data not shown).

Activation of the NF- κ B pathway was assessed by two criteria. Firstly, EMSA's were used to determine the ability of nuclear NF- κ B to bind to target DNA. Stimulation with LPS and TNF α , but not IFN γ , for 60 min stimulated DNA binding in control C6 cells but this was reduced by 85 \pm 16% (TNF α) and 90 \pm 11% (LPS) in A_{2A}AR-expressing cells (both p <0.05 *versus* control C6 cells, n=3; Figure 4A). Supershift analysis revealed that both bands constituted p50-p65 heterodimers (data not shown). To determine the functional consequences of reduced DNA binding, control and A_{2A}AR-expressing C6 cells were transfected with a 3- κ B enhancer conA-luciferase reporter construct to assess NF- κ B-mediated transcription. While TNF α treatment for 6 hr produced a 53.4 \pm 3.6-fold increase in luciferase activity (n=5) in control C6 cells, the fold-stimulation in A_{2A}AR-expressing C6 cells was only 4.3 \pm 2.7 (p <0.05 *versus* control C6 cells, n=5; Figure 4B). Therefore, A_{2A}AR expression selectively attenuated NF- κ B-dependent gene transcription and this was associated with a parallel reduction in NF- κ B binding to target DNA.

Effect of NF- κ B inhibition on iNOS induction Several studies examining the promoter elements that control iNOS gene transcription have revealed the presence of multiple κ B binding sites and demonstrated their importance for proper induction in response to inflammatory stimuli (Xie *et al.*, 1994; Taylor and Geller, 2000). Given that the effects of A_{2A}AR expression on p38 and JNK activation were minimal compared with the effect on NF- κ B function, it was likely that the inhibition of iNOS induction observed (Figure 1) could be accounted for by the A_{2A}AR's effects on the NF- κ B pathway. To test this hypothesis, C6 cells were pre-incubated with the NF- κ B inhibitor pyrrolidine

MOL1107

dithiocarbamate (PDTC) prior to 24 hr treatment with or without LPS/TNF α /IFN γ and assessment of nitrite accumulation in the medium (Dai *et al.*, 2003). Pre-incubation with PDTC attenuated nitrite accumulation by 55 \pm 7% (p <0.05, n =3) as compared with C6 cells pre-treated with an anti-oxidant control compound N-acetylcysteine (NACys) (Figure 5A). An alternative strategy was also employed to assess the effects of NF- κ B inhibition on nitrite accumulation. Specifically, control C6 cells were transfected with a wild type I κ B α expression construct prior to stimulation with LPS/TNF α /IFN γ (Figure 5B). Expression of recombinant I κ B α inhibits NF- κ B function by sequestering liberated NF- κ B dimers, thereby preventing their nuclear translocation and subsequent binding to target DNA (Sun *et al.*, 1996). Compared with vector-transfected C6 cells, nitrite accumulation was reduced by 68 \pm 15% in I κ B α -transfected cells (n =3, p <0.05, Figure 5B). Together, these data suggest that inhibition of NF- κ B caused by A_{2A}AR expression could at least partly explain the receptor's ability to attenuate iNOS induction.

Effect of A_{2A}AR expression on I κ B α regulation in C6 cells TNF α and LPS each activate NF- κ B by initiating the degradation of I κ B α , which allows p50-p65 heterodimers to translocate to the nucleus and initiate transcription following a series of phosphorylation and acetylation reactions on p65 (Karin *et al.*, 2004). I κ B α phosphorylation on serines 32 and 36 by the I κ B kinase (IKK) complex triggers its polyubiquitylation by the SCF ^{β TrCP} complex and subsequent degradation by the 26S proteasome. In control C6 cells, TNF α was able to initiate a marked reduction in I κ B α protein with similar kinetics to those observed by other investigators (Wang *et al.*, 1999; Figure 6A). However, in A_{2A}AR-expressing cells, the observed degradation of I κ B α in response to TNF α was significantly reduced (at 30 min, I κ B α reduction in control C6 cells was 84 \pm 12% versus 20 \pm 5% in A_{2A}AR-expressing C6 cells, p <0.05, n =3, Figure 6A). Immunoblotting with an antibody that specifically

MOL1107

recognised Ser³²Ser³⁶-phosphorylated IκBα revealed that this was associated with almost complete abolition of IκBα phosphorylation (phosphorylation following a 15 min exposure to TNFα reduced by some 83±8% in A_{2A}AR-expressing C6 cells *versus* controls, $p < 0.05$, $n = 3$, Figure 6A). A similar inhibition of IκBα degradation and phosphorylation was observed in response to LPS treatment, with Ser³²Ser³⁶ phosphorylation of IκBα after 15 min being reduced by 75±11% in A_{2A}AR-expressing C6 cells *versus* controls, $p < 0.05$, $n = 3$, (Figure 6B). Hence the ability of the A_{2A}AR to inhibit NF-κB activation in response to TNFα and LPS is likely due to inhibition of IκBα phosphorylation by the upstream IKK complex.

Effect of A_{2A}AR activation on monocyte adhesion to TNFα-stimulated HUVECs in vitro To determine whether the molecular mechanisms by which the A_{2A}AR inhibited inflammatory responses in C6 cells were conserved between different cell types, the effects of A_{2A}AR gene transfer were also assessed in HUVECs, a cell line whose responses to stimuli such as TNFα and LPS are well-characterised. Several reports have suggested that ECs express low levels of endogenous A_{2A}ARs (Sexl *et al.*, 1997; Wyatt *et al.*, 2002; Feoktistov *et al.*, 2002). To assess the ability of these receptors to inhibit inflammatory responses in HUVECs *in vitro*, cells were pretreated with a maximally effective concentration of the A_{2A}AR-selective agonist CGS21680 prior to treatment with increasing concentrations of TNFα and quantitation of U937 monocyte adhesion. While maximally effective concentrations of TNFα increased U937 adhesion by 148±25-fold ($n = 5$ experiments) with an EC₅₀ of 0.37±0.21 ng/ml, pretreatment with 5 μM CGS21680 increased the EC₅₀ to 2.00±0.88 ng/ml, thereby reducing monocyte adhesion at submaximal concentrations of TNFα (adhesion observed at 1 ng/ml TNFα reduced by 51±14% $n = 3$, by 5 μM CGS21680 *versus* vehicle-treated HUVECs, $p < 0.05$, Figure 7A,B). Pharmacological analysis of this effect

MOL1107

demonstrated that while the effect of CGS21680 was blocked completely by the A_{2A}AR-selective antagonist ZM241385, it could not be mimicked by the A₁AR-selective agonist CPA, indicative of an A_{2A}AR-mediated phenomenon (Figure 7B).

Effect of A_{2A}AR gene transfer on monocyte adhesion to TNF α -stimulated HUVECs in vitro

To assess whether it was possible to potentiate the anti-inflammatory effects of the A_{2A}AR, HUVECs were infected with recombinant AV encoding a myc epitope-tagged human A_{2A}AR with the aim of increasing receptor expression. The AV also expressed GFP from a separate open reading frame to facilitate identification of successfully infected cells by fluorescence microscopy. By this approach, it was possible to achieve recombinant protein expression in approximately 90% of infected HUVECs at optimal m.o.i.'s (Figure 8A) with A_{2A}AR expression reaching 0.34 \pm 0.06 pmol/mg protein (n=3 experiments) as determined by saturation binding analysis using ¹²⁵I-ZM241385 (Figure 8B). Interestingly, despite unequivocal identification of functional A_{2A}ARs (Figure 7), no specific binding of ¹²⁵I-ZM241385 was detectable in either uninfected or control AV/GFP-infected HUVECs. A similar inability to detect low level endogenous functional A_{2A}ARs by radioligand binding has also been reported for T-lymphocytes (Armstrong *et al.*, 2001).

Experiments performed in C6 cells suggested that A_{2A}AR expression was sufficient to inhibit inflammatory responses even in the absence of agonist. To determine whether this was also a feature of endothelial cells, U937 adhesion assays were performed on TNF α -treated HUVECs infected with either AV/GFP or AV/myc-humA_{2A}AR (Figure 9). While TNF α strongly promoted monocyte adhesion in control GFP-expressing cells, expression of the A_{2A}AR inhibited this effect by 84 \pm 8% (n=3, *p*<0.05 versus TNF α -treated HUVECs infected with control AV/GFP) and this was not improved substantially by the presence of the AR agonist NECA (89 \pm 8% inhibition, n=3, *p*<0.05 versus TNF α - and NECA-treated HUVECs infected with control AV/GFP, Figure 9).

MOL1107

Effect of A_{2A}AR gene transfer on E-selectin induction in HUVECs Adherence of leukocytes to inflamed endothelium is mediated by specific adhesion molecules on both cell types. E-selectin is a key molecule on the EC surface responsible for initial recruitment of leukocytes out of the circulation prior to their arrest and diapedesis into underlying tissue (Ley, 2001). In agreement with several other studies, exposure of control AV-infected HUVECs to either TNF α for 6 hr induced E-selectin expression at the cell surface (Oitzinger *et al.*, 2001; Figure 10A). A_{2A}AR gene transfer reduced the TNF α -mediated increase in cell surface E-selectin by 76 \pm 5% ($n=3$, $p<0.05$ versus TNF α -treated AV/GFP-infected HUVECs, Figure 10A). Moreover, this effect was not restricted to TNF α , as induction of E-selectin following a 4 hr stimulation with LPS was similarly reduced (80 \pm 12%, $n=3$, $p<0.05$ versus LPS-treated AV/GFP-infected HUVECs, Figure 10B) as determined by immunoblotting. Thus, A_{2A}AR expression is sufficient to inhibit both E-selectin induction and monocyte adhesion.

Effect of NF- κ B inhibition on E-selectin induction and monocyte adhesion Analysis of the human E-selectin promoter has identified four positive regulatory domains (termed PDI to IV) responsible for conferring induction in response to inflammatory stimuli (Read *et al.*, 1997). PDs I, III and IV are κ B-binding sites while PDII is an AP-1 site at which an ATF2/c-jun heterodimer is constitutively bound. Thus, maximal induction arises from occupation of the κ B-binding sites by NF- κ B as well as p38- and JNK-mediated phosphorylation of ATF2 and c-jun respectively (Read *et al.*, 1997). The ability of TNF α to promote E-selectin induction in HUVECs was found to be dependent on κ B binding rather than AP-1 activation, as HUVEC pretreatment with the NF- κ B inhibitor PDTC inhibited induction by 87 \pm 10% under conditions in which the p38 inhibitor SB203580 had no significant effect (7 \pm 16% increase versus non-pretreated cells, $p>0.05$ NS, $n=3$, Figure 11A). Importantly, the effect of PDTC could not be explained by its anti-oxidant properties, since parallel treatment with the anti-oxidant NAcCys had minimal effects on E-selectin

MOL1107

induction ($6\pm 10\%$ increase *versus* non-pretreated cells, $p > 0.05$ NS, $n=3$, Figure 11A). Consistent with other investigators (Read *et al.*, 1997), inhibition of the ERK signalling pathway using the MEK inhibitor U0126 also had no effect on induction ($6\pm 7\%$ increase *versus* non-pretreated cells, $p > 0.05$ NS, $n=3$, Figure 11A). Again, to confirm a role for NF- κ B, HUVECs were transfected with a WT I κ B α expression construct prior to stimulation with TNF α and measurement of E-selectin induction. These experiments demonstrated that compared with vector-transfected cells, I κ B α expression reduced TNF α -stimulated E-selectin induction by $72\pm 7\%$ ($n=3$, $p < 0.05$ *versus* vector-transfected controls, Figure 11B). Importantly, the observed reduction in E-selectin observed following inhibition of NF- κ B was associated with a parallel inhibition of U937 adhesion to TNF α -stimulated HUVECs *in vitro* (PDTC produced a $88\pm 9\%$ *versus* $25\pm 10\%$ inhibition of adhesion in NAcCys-treated cells, $n=4$, $p < 0.05$, Figure 11C).

Effect of A_{2A}AR gene transfer on NF- κ B regulation in HUVECs The above experiments demonstrated that, similarly to C6 glioma cells, the anti-inflammatory effects of the A_{2A}AR in HUVECs could be largely mimicked by inhibition of NF- κ B signalling. To determine whether A_{2A}AR gene transfer could also inhibit NF- κ B binding to target DNA in HUVECs, EMSAs were performed on TNF α -treated cells following infection with either AV/GFP or AV/myc-humA_{2A}AR (Figure 12A). These demonstrated that the ability of TNF α to promote p50-p65 heterodimer binding to target DNA was reduced by $86\pm 15\%$ upon A_{2A}AR gene transfer ($n=5$, $p < 0.05$ *versus* TNF α -treated AV/GFP-infected HUVECs, Figure 12A).

Translocation of NF- κ B to the nucleus is triggered by the phosphorylation-dependent degradation of the I κ B proteins that maintain NF- κ B in the cytoplasm (Karin *et al.*, 2004). Expression of the A_{2A}AR in C6 cells severely attenuated I κ B α phosphorylation on Ser³² and Ser³⁶, the two sites whose phosphorylation by the IKK complex is required for

MOL1107

polyubiquitination and subsequent degradation by the proteasome (Figure 6). However, despite unequivocal evidence of AV-directed $A_{2A}AR$ expression in HUVECs, the ability of $TNF\alpha$ to trigger the degradation of $I\kappa B\alpha$ was unaffected (degradation compared with vehicle-treated control at 15 min was $94\pm 6\%$ (AV/GFP) *versus* $89\pm 10\%$ (AV/myc-hum $A_{2A}AR$), $n=3$, $p>0.05$, NS; Figure 12B), suggesting that the mechanisms by which the $A_{2A}AR$ inhibits NF- κB signalling differ between C6 glioma and HUVEC systems.

To determine whether the nuclear translocation of NF- κB was altered despite normal $I\kappa B\alpha$ degradation, confocal laser-scanning microscopy was performed to analyse the subcellular distribution of p65 in AV-infected HUVECs following treatment with or without $TNF\alpha$ (Figure 12C). Under unstimulated conditions, p65 resided in the cytoplasm in both sets of AV-infected cells. However, while stimulation with $TNF\alpha$ promoted the nuclear translocation of p65 in controls, p65 was excluded from the nucleus of $A_{2A}AR$ -expressing HUVECs (Figure 12C). Hence, $A_{2A}AR$ gene transfer in HUVECs profoundly inhibits the ability of NF- κB p50-p65 heterodimers to bind target DNA and this is associated with a parallel reduction in p65 translocation to the nucleus in the absence of any effect on $I\kappa B\alpha$ degradation

MOL1107

DISCUSSION

The A_{2A}AR has been identified as a protective anti-inflammatory receptor protein not only from numerous pharmacological studies (reviewed in Linden, 2001) but also from characterisation of inflammatory responses in mice in which both copies of the A_{2A}AR gene have been deleted (Ohta and Sitkovsky, 2001). Gene dosage studies have provided evidence to show that, at least in T-lymphocytes, there is no A_{2A}AR reserve (Armstrong *et al.*, 2001). Consequently, pathophysiological conditions that alter A_{2A}AR expression, such as the onset of hypoxia (Kobayashi and Millhorn, 1999) and EC exposure to Th1 cytokines (Nguyen *et al.*, 2003), are likely to alter cellular responsiveness to inflammatory stimuli. However, despite unequivocal evidence of its potent anti-inflammatory properties across different cell types, the molecular basis for the A_{2A}AR's anti-inflammatory effects have not been examined in detail. To begin addressing some of these issues, we have focused on characterising the effects of increasing A_{2A}AR expression on glial and EC model systems, each of which are associated with multiple inflammatory diseases.

iNOS induction is a well-characterised marker of glial cell inflammation (Brown and Bal-Price, 2003). Stable expression of the A_{2A}AR in C6 glioma cells was sufficient to abolish induction of iNOS expression and NF-κB activation. Moreover, this abolition did not require the presence of agonist and was not reversed by pre-incubation with the A_{2A}AR-selective antagonist ZM241385, suggesting that in this system the receptor displays some agonist-independent basal activity. A similar phenomenon was also observed for monocyte adhesion, E-selectin induction and NF-κB activation in HUVECs upon A_{2A}AR expression to a level of only 0.3-0.4 pmol/mg, suggesting that agonist-independent signalling may be an intrinsic property of the A_{2A}AR. Consistent with this hypothesis, constitutive A_{2A}AR activation of either cAMP production or the ERK pathway in the absence of agonist has

MOL1107

been observed in other studies (Ledent *et al.*, 1992; Klinger *et al.*, 2002). However, both this study and others describing agonist-independent signalling from the A_{2A}AR have been cell systems in which the recombinant receptor is overexpressed. Therefore, the physiological significance *in vivo* of any basal activity of endogenous A_{2A}ARs expressed at low levels is unclear and will require the development of an A_{2A}AR-selective inverse agonist. Despite this caveat, when considered in the context of our observations the increases in A_{2A}AR expression and function seen upon cytokine treatment or hypoxia in multiple cell types (Kobayashi and Millhorn, 1999; Khoa *et al.*, 2001; Nguyen *et al.*, 2003) likely constitute important negative feedback mechanisms that prevent the development of an excessive and inappropriate inflammatory response. The availability of A_{2A}AR-deficient mice can now allow quantitative assessment of the presence and importance of such a negative feedback loop in individual inflammatory cells.

A major finding from our experiments was that the pronounced inhibition of TNF α - and LPS-mediated inflammatory responses could be explained by a suppressive effect of A_{2A}AR expression specifically on the NF- κ B pathway rather than the parallel p38 and JNK stress-activated kinase modules. However, while expression of the A_{2A}AR in glial cells blocked the IKK-mediated I κ B α phosphorylation on Ser³² and Ser³⁶ that triggers its degradation, I κ B α degradation was unaffected upon A_{2A}AR expression in endothelial cells. Thus, the A_{2A}AR is able to inhibit the NF- κ B pathway at multiple post-receptor loci common to TNF α and LPS/Toll-like receptor 4 (TLR4) signalling. In C6 cells, this locus must reside at a site at which TLR4 and TNF receptor signalling converge to activate NF- κ B. The most likely candidates include components of the IKK complex (particularly IKK β and IKK γ /NEMO) as well as any IKK kinases activated by both LPS and TNF α .

In terms of receptor pharmacology, we found that activation of endogenous A_{2A}ARs on HUVECs by the selective agonist CGS21680 was able to significantly inhibit

MOL1107

monocyte adhesion whereas the non-selective AR agonist NECA was not (Figures 7 and 9). At the concentration used (5 μ M), NECA activates all four AR subtypes (Fredholm *et al.*, 2001). Several studies have demonstrated that both A_{2A} and A_{2B}ARs are predominantly expressed in endothelial cells. While both receptors share an ability to elevate cAMP levels *via* interaction with G_s, the A_{2B}AR can also couple to G_{q/11} to mobilise intracellular calcium (Feoktistov & Biaggioni, 1997). This additional signalling capacity accounts for its reported ability to induce the expression of angiogenic factors from endothelial cells under conditions where the A_{2A}AR does not (Feoktistov *et al.*, 2002). Consequently, upon exposure to NECA, A_{2B}AR activation may counteract the simultaneous effects of A_{2A}AR activation under the same conditions and this may explain why only CGS21680 reduces the adhesion observed at maximally effective concentrations of TNF α .

Some of the findings in HUVECs presented here are consistent with the recent observations of Majumdar and Aggarwal (2003), who described an adenosine-mediated inhibition of NF- κ B in several cell types, including HeLa and cultured endothelial cells. Pharmacological analysis ruled out a contribution of A₁ and A₃ARs but did not address the specific involvement of A_{2A} or A_{2B}ARs in each of the cell types under investigation (Majumdar & Aggarwal, 2003). However, the data presented here would suggest that the A_{2A}AR subtype may be largely responsible for the inhibition of NF- κ B observed by these investigators. A particularly important finding from Majumdar & Aggarwal (2003) was that adenosine specifically inhibited TNF α -induced NF- κ B activation and nuclear translocation in the absence of any effect on I κ B degradation, which is consistent with our observations in A_{2A}AR-expressing HUVECs. However, in contrast to their results, we found that A_{2A}AR expression blocked NF- κ B-mediated induction of E-selectin by both TNF α and LPS, suggestive of an effect of the A_{2A}AR on the NF- κ B nuclear translocation process that is common to both TNFR1 and TLR4 signalling cascades. This could be either reduced

MOL1107

nuclear import of p50-p65 heterodimers and/or accelerated CRM1-mediated export of I κ B α /NF- κ B complexes out of the nucleus (Arenzana-Seisdedos *et al.*, 1997).

A_{2A}AR activation elevates intracellular cAMP levels in HUVECs *via* interaction with G_s and stimulation of adenylyl cyclase (Klinger *et al.*, 2002). Consistent with other investigators, we have noted that elevation of cAMP in endothelial cells is sufficient to ameliorate κ B-dependent inflammatory responses, including adhesion molecule induction and subsequent monocyte adhesion (Morandini *et al.*, 1996; Sands and Palmer, unpublished observations). However, the mechanisms by which this occurs appear to vary depending on the nature of the cAMP-elevating stimulus. For example, cyclic AMP-responsive element binding protein (CREB), which is phosphorylated on Ser¹³³ and activated upon elevation of intracellular cyclic AMP levels, can directly block NF- κ B-induced transcription without altering nuclear translocation or DNA binding by recruiting the transcriptional co-activator CREB-binding protein (CBP), thereby reducing the number of transcriptionally competent CBP/NF- κ B complexes (Parry and Mackman, 1997). In contrast, the cAMP-elevating hormone adiponectin inhibits NF- κ B responses in ECs by inhibiting IKK-mediated I κ B phosphorylation and degradation (Ouchi *et al.*, 2000). The data from this study and Majumdar & Aggarwal (2003) both argue that despite being able to elevate cAMP levels in HUVECs (Klinger *et al.*, 2002), the A_{2A}AR inhibits NF- κ B in these cells *via* a unique mechanism distinct from those employed by forskolin and adiponectin.

It should be noted, however, that despite the profound inhibitory effects of A_{2A}AR on NF- κ B reported here, this is unlikely to be the only mechanism by which this receptor blocks inflammatory responses. A clue as to other potential mechanisms is suggested by our observation that while A_{2A}AR expression abolishes iNOS-mediated nitrite accumulation in response to LPS/TNF α /IFN γ treatment (Figure 1), inhibition of NF- κ B signalling by either PDTC pretreatment or expression of I κ B α fails to completely block this effect (Figure 5).

MOL1107

Functional analysis of iNOS promoters in multiple species have revealed the presence of GAS sites, which bind activated STAT1 dimers, and interferon-regulatory factor-1 (IRF-1) sites (Teng *et al.*, 2002). Thus, complete inhibition of iNOS induction by the A_{2A}AR may also require inhibition of IFN γ signalling as well as NF- κ B, an issue that we are currently addressing.

In conclusion, we have consolidated and extended previous studies investigating the anti-inflammatory effects of adenosine. Specifically, we have demonstrated that increasing expression of the A_{2A}AR subtype suppresses NF- κ B activation in two inflammatory cell types *via* distinct molecular mechanisms. The ability to specifically inhibit NF- κ B activation *via* multiple routes is likely to be an important reason why the A_{2A}AR can exert its inhibitory effects even when cell type-specific mechanisms are in place to regulate NF- κ B activation. In addition, the pronounced suppression of inflammatory responses seen upon A_{2A}AR gene transfer in our studies provide a complimentary counterpoint to the marked enhancement of inflammatory responses produced upon homozygous deletion of the A_{2A}AR *in vivo*, and suggests that the A_{2A}AR acts as a rheostat whose expression controls cellular responsiveness to NF- κ B-mobilising stimuli. As such, our observations further underscore the importance of the A_{2A}AR as both a key target for generation of anti-inflammatory therapeutics for a wide range of disorders (Linden, 2001; Sitkovsky *et al.*, 2004) and a protein whose defective regulation may influence the pathophysiology of diseases associated with either immune deficiency or suppression. Finally, the availability of model systems described herein that permit assessment of the anti-inflammatory signalling capacity of recombinant A_{2A}ARs *in vitro* can now allow a rigorous analysis of how changes in receptor phosphorylation and subcellular distribution in response to agonists or other stimuli (Palmer and Stiles, 1999; Burgueno *et al.*, 2003) influence the magnitude and/or kinetics of the receptor's potent anti-inflammatory effects.

MOL1107

FOOTNOTE

This work was supported by project grants from the British Heart Foundation and National Heart Research Fund, equipment grants from Tenovus-Scotland and The Wellcome Trust (TMP) and studentships from the Medical Research Council (AFM) and British Heart Foundation (EWS).

Reprint requests should be addressed to: T.M. Palmer, Ph.D., 425 Davidson Bldg., University of Glasgow, Glasgow G12 8QQ, Scotland, U.K.

MOL1107

REFERENCES

Arenzana-Seisdedos F, Turpin P, Rodriguez M, Thomas D, Hay RT, Virelizier JL and Dargemont C (1997) Nuclear localization of I κ B α promotes active transport of NF- κ B from the nucleus to the cytoplasm. *J. Cell Sci.* **110**:369-378.

Armstrong JM, Chen JF, Schwarzschild MA, Apasov S, Smith PT, Caldwell C, Chen P, Figler H, Sullivan G, Fink S, Linden J and Sitkovsky M (2001) Gene dose effect reveals no G_s-coupled A_{2A} adenosine receptor reserve in murine T-lymphocytes: studies of cells from A_{2A}-receptor-gene-deficient mice. *Biochem. J.* **354**:123-130.

Banerjee SK, Young HW, Volmer JB and Blackburn MR (2002) Gene expression profiling in inflammatory airway disease associated with elevated adenosine. *Am. J. Physiol. Lung Cell Mol. Physiol.* **282**:L169-182.

Bouma MG, van den Wildenberg FA and Buurman WA (1996) Adenosine inhibits cytokine release and expression of adhesion molecules by activated human endothelial cells. *Am. J. Physiol.* **270**:C522-C529.

Brown GC and Bal-Price A (2003) Inflammatory neurodegeneration mediated by nitric oxide, glutamate, and mitochondria. *Mol. Neurobiol.* **27**:325-355.

Burgueno J, Blake DJ, Benson MA, Tinsley CL, Esapa CT, Canela EI, Penela P, Mallol J, Mayor F Jr, Lluís C, Franco R and Ciruela F (2003) The adenosine A_{2A} receptor interacts with the actin-binding protein α -actinin. *J. Biol. Chem.* **278**:37545-37552.

MOL1107

Cronstein BN, Montesinos MC and Weissmann G (1999) Salicylates and sulfasalazine, but not glucocorticoids, inhibit leukocyte accumulation by an adenosine-dependent mechanism that is independent of inhibition of prostaglandin synthesis and p105 of NF- κ B. *Proc. Nat'l. Acad. Sci. U.S.A.* **96**:6377-6381.

Dai Y, Rahmani M and Grant S (2003) Proteasome inhibitors potentiate leukemic cell apoptosis induced by the cyclin-dependent kinase inhibitor flavopiridol through a SAPK/JNK- and NF- κ B-dependent process. *Oncogene* **22**:7108-7122.

Felsch A, Stocker K and Borchard U (1995) Phorbol ester-stimulated adherence of neutrophils to endothelial cells is reduced by adenosine A₂ receptor agonists. *J. Immunol.* **155**:333-338.

Feoktistov I and Biaggioni I (1997) Adenosine A_{2B} receptors. *Pharmacol Rev.* **49**:381-402.

Feoktistov I, Goldstein AE, Ryzhov S, Zeng D, Belardinelli L, Voyno-Yasenetskaya T and Biaggioni I (2002) Differential expression of adenosine receptors in human endothelial cells: role of A_{2B} receptors in angiogenic factor regulation. *Circ. Res.* **90**:531-538.

Fredholm BB, Ijzerman AP, Jacobson KA, Klotz KN and Linden J (2001) International Union of Pharmacology XXV. Nomenclature and classification of adenosine receptors. *Pharmacol. Rev.* **53**:527-552.

Ghosh S and Karin M. (2002) Missing pieces in the NF- κ B puzzle. *Cell* **109**:S81-96.

MOL1107

He TC, Zhou S, da Costa LT, Yu J, Kinzler KW and Vogelstein B (1998) A simplified system for generating recombinant adenoviruses. *Proc. Nat'l. Acad. Sci. U.S.A.* **95**:2509-2514.

Hevel JM and Marletta MA (1994) Nitric-oxide synthase assays. *Methods Enzymol.* **233**:250-258.

Hirsch EC, Breidert T, Rousselet E, Hunot S, Hartmann A and Michel PP (2003) The role of glial reaction and inflammation in Parkinson's disease. *Ann. N.Y. Acad. Sci.* **991**:214-228.

Jin X, Shepherd RK, Duling BR and Linden J (1997) Inosine binds to A₃ adenosine receptors and stimulates mast cell degranulation. *J. Clin. Invest.* **100**:2849-2857.

Karin M, Yamamoto Y and Wang QM (2004) The IKK NF- κ B system: a treasure trove for drug development. *Nat. Rev. Drug Discov.* **3**:17-26.

Khoa ND, Montesinos MC, Reiss AB, Delano D, Awadallah N and Cronstein BN (2001) Inflammatory cytokines regulate function and expression of adenosine A_{2A} receptors in human monocytic THP-1 cells. *J. Immunol.* **167**:4026-4032.

Klinger M, Kuhn M, Just H, Stefan E, Palmer T, Freissmuth M and Nanoff C (2002) Removal of the carboxy terminus of the A_{2A}-adenosine receptor blunts constitutive activity:

MOL1107

differential effect on cAMP accumulation and MAP kinase stimulation. *Naunyn Schmiedebergs Arch. Pharmacol.* **366**:287-298.

Kobayashi S, Millhorn DE (1999) Stimulation of expression for the adenosine A_{2A} receptor gene by hypoxia in PC12 cells: a potential role in cell protection. *J. Biol. Chem.* **274**:20358-20365.

Kumar S, Boehm J and Lee JC (2003) p38 MAP kinases: key signalling molecules as therapeutic targets for inflammatory diseases. *Nat. Rev. Drug Discov.* **2**:717-726.

Ledent C, Dumont JE, Vassart G, and Parmentier M (1992) Thyroid expression of an A₂ adenosine receptor transgene induces thyroid hyperplasia and hyperthyroidism. *EMBO J.* **11**:537-42.

Ley K (2001) Pathways and bottlenecks in the web of inflammatory adhesion molecules and chemoattractants. *Immunol. Res.* **24**:87-95.

Linden J (2001) Molecular approach to adenosine receptors: receptor-mediated mechanisms of tissue protection. *Annu. Rev. Pharmacol. Toxicol.* **41**:775-787.

Majumdar S and Aggarwal BB (2003) Adenosine suppresses activation of nuclear factor- κ B selectively induced by tumor necrosis factor in different cell types. *Oncogene* **22**:1206-1218.

MOL1107

Manning AM and Davis RJ (2003) Targeting JNK for therapeutic benefit: from junk to gold? *Nat. Rev. Drug Discov.* **2**:554-565.

Monsonogo A and Weiner HL (2003) Immunotherapeutic approaches to Alzheimer's disease. *Science* **302**:834-838.

Montesinos MC, Yap JS, Desai A, Posadas I, McCrary CT and Cronstein BN (2000) Reversal of the antiinflammatory effects of methotrexate by the nonselective adenosine receptor antagonists theophylline and caffeine: evidence that the antiinflammatory effects of methotrexate are mediated *via* multiple adenosine receptors in rat adjuvant arthritis. *Arthritis Rheum.* **43**:656-663.

Morandini R, Ghanem G, Portier-Lemarie A, Robaye B, Renaud A and Boeynaems JM (1996) Action of cAMP on expression and release of adhesion molecules in human endothelial cells. *Am. J. Physiol.* **270**:H807-816.

Nguyen DK, Montesinos MC, Williams AJ, Kelly M and Cronstein BN (2003) Th1 cytokines regulate adenosine receptors and their downstream signaling elements in human microvascular endothelial cells. *J. Immunol.* **171**:3991-3998.

Ohta A and Sitkovsky M (2001) Role of G-protein-coupled adenosine receptors in downregulation of inflammation and protection from tissue damage. *Nature* **414**:916-920.

MOL1107

Oitzinger W, Hofer-Warbinek R, Schmid JA, Koshelnick Y, Binder BR and de Martin R. (2001) Adenovirus-mediated expression of a mutant I κ B kinase 2 inhibits the response of endothelial cells to inflammatory stimuli. *Blood* **97**:1611-1617.

Ouchi N, Kihara S, Arita Y, Okamoto Y, Maeda K, Kuriyama H, Hotta K, Nishida M, Takahashi M, Muraguchi M, Ohmoto Y, Nakamura T, Yamashita S, Funahashi T and Matsuzawa Y (2000) Adiponectin, an adipocyte-derived plasma protein, inhibits endothelial NF- κ B signaling through a cAMP-dependent pathway *Circulation* **102**:1296-1301.

Palmer TM, Poucher SM, Jacobson KA, and Stiles GL (1995) ¹²⁵I-4-(2-[7-amino-2-[2-furyl][1,2,4]triazolo[2,3-a][1,3,5] triazin-5-yl-amino]ethyl)phenol, a high affinity antagonist radioligand selective for the A_{2A} adenosine receptor. *Mol. Pharmacol.* **48**:970-974.

Palmer TM and Stiles GL (1999) Stimulation of A_{2A} adenosine receptor phosphorylation by protein kinase C activation: evidence for regulation by multiple protein kinase C isoforms. *Biochemistry* **38**:14833-14842.

Parry GC and Mackman N (1997) Role of cyclic AMP response element-binding protein in cyclic AMP inhibition of NF- κ B-mediated transcription. *J. Immunol.* **159**:5450-5456.

Read MA, Whitley MZ, Gupta S, Pierce JW, Best J, Davis RJ and Collins T (1997) Tumor necrosis factor alpha-induced E-selectin expression is activated by the nuclear factor- κ B

MOL1107

and c-JUN N-terminal kinase/p38 mitogen-activated protein kinase pathways. *J. Biol. Chem.* **272**:2753-27561.

Sexl V, Mancusi G, Holler C, Gloria-Maercker E, Schutz W and Freissmuth M (1997) Stimulation of the mitogen-activated protein kinase *via* the A_{2A}-adenosine receptor in primary human endothelial cells. *J. Biol. Chem.* **272**:5792-5799.

Sitkovsky MV, Lukashev D, Apasov S, Kojima H, Koshiba M, Caldwell C, Ohta A and Thiel M (2004) Physiological control of immune response and inflammatory tissue damage by hypoxia-inducible factors and adenosine A_{2A} receptors. *Annu. Rev. Immunol.* **22**:657-682.

Sun S, Elwood J and Greene WC (1996) Both amino- and carboxyl-terminal sequences within IκBα regulate its inducible degradation. *Mol. Cell Biol.* **16**:1058-1065.

Taylor BS and Geller DA (2000) Molecular regulation of the human inducible nitric oxide synthase (iNOS) gene. *Shock* **13**:413-424.

Teng X, Zhang H, Snead C and Catravas JD (2002) Molecular mechanisms of iNOS induction by IL-1 β and IFN-γ in rat aortic smooth muscle cells. *Am. J. Physiol. Cell Physiol.* **282**:C144-C152.

Wang CN, Shiao YJ, Lin YL and Chen CF (1999) Nepalolide A inhibits the expression of inducible nitric oxide synthase by modulating the degradation of IκB-α and IκB-β in C6 glioma cells and rat primary astrocytes. *Br. J. Pharmacol.* **128**:345-356.

MOL1107

Wyatt AW, Steinert JR, Wheeler-Jones CP, Morgan AJ, Sugden D, Pearson JD, Sobrevia L and Mann GE. (2002) Early activation of the p42/p44MAPK pathway mediates adenosine-induced nitric oxide production in human endothelial cells: a novel calcium-insensitive mechanism. *FASEB J.* **12**:1584-1594.

Xie QW, Kashiwabara Y and Nathan C (1994) Role of transcription factor NF- κ B/Rel in induction of nitric oxide synthase. *J. Biol. Chem.* **269**:4705-4708.

MOL1107

FIGURE LEGENDS

Figure 1 Effect of A_{2A}AR expression on nitrite accumulation and iNOS induction in C6 glioma cells

Panel A: Control and A_{2A}AR-expressing C6 cells were treated for 24 hr with 1 µg/ml LPS (L), 10 ng/ml TNFα (T) or 10 units/ml IFNγ (I) individually or in combination (C=LPS/TNFα/IFNγ) prior to analysis of nitrite accumulation as described in the Materials and Methods. This is one of multiple similar experiments.

Panel B: Control and A_{2A}AR-expressing C6 cells were treated for 24 hours with or without LPS/TNFα/IFNγ in the absence or presence of 5 µM NECA. Detergent-soluble extracts from treated cells were then normalised for protein content prior to fractionation by SDS-PAGE and assessment of iNOS and A_{2A}AR expression by immunoblotting. This is one of multiple similar experiments.

Panel C: Control and A_{2A}AR-expressing C6 cells were treated for 24 hours with or without LPS/TNFα/IFNγ in the absence or presence of 1 µM ZM241385 as indicated. Samples were then analysed for nitrite accumulation as described in the Materials and Methods. This is one of multiple similar experiments.

Figure 2 Effect of conditioned medium from A_{2A}AR-expressing C6 glioma cells on iNOS induction in control C6 glioma cells

Fresh medium was added to confluent dishes of control and A_{2A}AR-expressing C6 cells. After 24 hours, the medium from each dish was removed, supplemented with or without LPS/TNFα/IFNγ, and added to confluent monolayers of control C6 cells for a further 24 hours as described in Figure 1. Protein-normalised soluble extracts were then prepared and

MOL1107

fractionated by SDS-PAGE for immunoblot analysis of iNOS induction. This is one of multiple experiments.

Figure 3 Effect of A_{2A}AR expression on TNF α stimulation of p38 phosphorylation and JNK activation in C6 glioma cells

Panel A: Control and A_{2A}AR-expressing C6 glioma cells were treated with or without 10 ng/ml TNF α or 5 μ g/ml anisomycin for the indicated times prior to preparation of soluble cell extracts. Following normalisation for protein content, duplicate samples were fractionated by SDS-PAGE and transferred to nitrocellulose for parallel immunoblotting with Thr¹⁸⁰/Tyr¹⁸²phospho-specific and total anti-p38 antibodies as described in the Materials and Methods.

Panel B: Control and A_{2A}AR-expressing C6 glioma cells were treated with or without 10 ng/ml TNF α or 5 μ g/ml anisomycin for the indicated times prior to preparation of soluble cell extracts. Following normalisation for protein content, samples were assayed for JNK activation by incubation with glutathione-Sepharose-bound GST-c-Jun(1-79) and assay of the pulled down kinase. Phosphorylation of GST-c-Jun(1-79) was assessed by SDS-PAGE and immunoblotting with a Ser⁶³phospho-specific c-Jun antibody and parallel immunoblotting of treated cell extracts with anti-JNK1,2 antibody as described in the Materials and Methods.

Figure 4 Effect of A_{2A}AR expression on NF- κ B activation in C6 glioma cells

Panel A: Control and A_{2A}AR-expressing C6 glioma cells were treated with or without 10 ng/ml TNF α , 1 μ g/ml LPS or 10 units/ml IFN γ for 60 min prior to isolation of nuclei for EMSA analysis with a κ B-selective oligonucleotide probe as described in the Materials and Methods. This is one of multiple experiments.

MOL1107

Panel B: Control and A_{2A}AR-expressing C6 glioma cells were co-transfected with a κ B-luciferase reporter construct and pSV β -galactosidase. Forty eight hours post-transfection, cells were treated with or without TNF α as indicated and extracts prepared for assay of luciferase and β -galactosidase activities and normalisation with respect to transfection efficiency and protein content as described in the Materials and Methods. This is one of multiple experiments.

Figure 5 Effect of NF- κ B inhibition on nitrite accumulation in C6 glioma cells

Panel A: Control C6 glioma cells were pretreated with or without 100 μ M PTDC or NAcCys for 30 min prior to the addition of vehicle or LPS/TNF α /IFN γ for a further 24 hours as indicated. Medium from treated cells was then analysed for nitrite accumulation as described in the Materials and Methods. This is one of multiple experiments.

Panel B: Control C6 glioma cells were transfected with either pcDNA3 vector or pcDNA3/HA-tagged WT I κ B α as indicated. Twenty four hours post-transfection, cells were treated with LPS/TNF α /IFN γ for a further 24 hours as indicated. Medium from treated cells was then analysed for nitrite accumulation as described in the Materials and Methods. This is one of multiple experiments.

Figure 6 Effect of A_{2A}AR expression on agonist-stimulated I κ B α phosphorylation and degradation in C6 glioma cells

Panel A: Control and A_{2A}AR-expressing C6 glioma cells were treated with or without 10 ng/ml TNF α for the indicated times prior to preparation of detergent-soluble extracts. Samples equalised for protein content were fractionated by SDS-PAGE for immunoblotting with anti-I κ B α (*Upper*) or anti-Ser³²Ser³⁶phospho-I κ B α (*Lower*) antibodies as described in the Materials and Methods. This is one of multiple experiments.

MOL1107

Panel B: Control and A_{2A}AR-expressing C6 glioma cells were treated with or without 1 µg/ml LPS for the indicated times prior to preparation of detergent-soluble extracts. Samples equalised for protein content were fractionated by SDS-PAGE for immunoblotting with anti-IκBα (*Upper*) or anti-Ser³²Ser³⁶phospho-IκBα (*Lower*) antibodies as described above. This is one of multiple experiments.

Figure 7 Effect of endogenous A_{2A}AR activation on monocyte adhesion to TNFα stimulated HUVECs *in vitro*

Panel A: Confluent HUVEC monolayers were pretreated for 30 min with 5 µM CGS21680 prior to incubation with increasing concentrations of TNFα for 6 hours as indicated. U937 promonocytic cells were then overlaid and the number of adherent cells quantitated as described in the Materials and Methods. This is one of multiple experiments.

Panel B: Confluent HUVEC monolayers were pretreated for 30 min with 5 µM CGS21680 (CGS), 5 µM CGS21680 and 1 µM ZM241385 (CGS+ZM) or 5 µM N⁶-cyclopentyladenosine (CPA) as indicated prior to treatment with or without 10 ng/ml TNFα for 6 hours and assessment of U937 adhesion as described in the Materials and Methods. This is one of multiple experiments.

Figure 8 Adenovirus-directed expression of the human A_{2A}AR in HUVECs

Panel A: HUVECs were infected with AV/myc-human A_{2A}AR at the indicated m.o.i. as described in the Materials and Methods. Following the isolation of detergent-soluble extracts, samples were equalised for protein content and fractionated by SDS-PAGE for immunoblotting with anti-myc epitope antibody 9E10 to specifically identify recombinant receptor. Blots were then stripped and reprobed with an antibody versus G_iα-2, to ensure equivalent protein loading in each lane. Determination of “% cells infected” was derived

MOL1107

from counting the number of GFP-expressing cells by fluorescence microscopy and the total number of cells by light microscopy within five different fields. This is one of multiple experiments.

Panel B: Membranes prepared from HUVECs infected with 25 pfu/cell AV/myc-human A_{2A}AR were subjected to saturation binding analysis using the A_{2A}AR-selective antagonist radioligand ¹²⁵I-ZM241385 as described in the Materials and Methods. This is one of multiple experiments.

Figure 9 Effect of A_{2A}AR gene transfer on monocyte adhesion to TNF α -pretreated HUVECs *in vitro*

HUVECs were infected with AV/myc-human A_{2A}AR at an m.o.i. of 25 pfu/cell as described in the Materials and Methods. Following pretreatment for 30 min with or without 5 μ M NECA, cells were incubated with 10 ng/ml TNF α for 6 hours as indicated. U937 cells were then overlaid and the number of adherent cells quantitated as described in the Materials and Methods. This is one of multiple experiments.

Figure 10 Effect of A_{2A}AR gene transfer on TNF α - and LPS-mediated induction of E-selectin expression

Panel A: HUVECs were infected with either AV/GFP (control AV) or AV/myc-human A_{2A}AR at an m.o.i. of 25 pfu/cell as described in the Materials and Methods. Following pretreatment with or without 10 ng/ml TNF α for 6 hours, cell surface E-selectin expression was determined by ELISA as described in the Materials and Methods. This is one of multiple experiments.

Panel B: HUVECs were infected with either AV/GFP (control AV) or AV/myc-human A_{2A}AR at an m.o.i. of 25 pfu/cell as described in the Materials and Methods. Following

MOL1107

treatment in the absence (0) or presence of 1 $\mu\text{g/ml}$ LPS either alone (LPS) or with 5 μM NECA (LPS+N) for 4 hours, cell surface E-selectin expression was determined by immunoblotting as described in the Materials and Methods. This is one of multiple experiments.

Figure 11 Effect of NF- κ B inhibition on TNF α -mediated induction of E-selectin and monocyte adhesion in HUVECs

Panel A: Confluent HUVECs in a 96-well plate were incubated with or without 10 ng/ml TNF α following a 30 min preincubation in the absence or presence of 10 μM SB203580, 10 μM U0126, 100 μM PDTC or 100 μM NAcCys. Quantitation of E-selectin induction was by ELISA as described the in the Materials and Methods. This is one of multiple experiments.

Panel B: HUVECs were transfected with pMaxGFP and either pcDNA3 vector or pcDNA3/HA-tagged WT I κ B α , seeded into a 96-well plate and cultured for forty eight hours as described in the Materials and Methods. Cells were then treated with or without 10 ng/ml TNF α for 6 hr prior to quantitation of E-selectin induction by ELISA. This is one of multiple experiments.

Panel C: Confluent HUVEC monolayers were pretreated for 30 min with either 100 μM PDTC or NAcCys as indicated prior to stimulation with 10 ng/ml TNF α for 6 hours. U937 cells were then overlaid and the number of adherent cells quantitated as described the Materials and Methods. This is one of multiple experiments.

Figure 12 Effect of A_{2A}AR gene transfer on the regulation of NF- κ B in HUVECs

Panel A: Confluent HUVECs were treated for 60 min in the absence of presence of 10 ng/ml TNF α prior to isolation of nuclei for incubation with a κ B-selective oligonucleotide probe

MOL1107

and the indicated antibodies for EMSA analysis as described in the Materials and Methods. The *asterix* indicates a non-specifically labelled band. This is one of multiple experiments.

Panel B: Confluent HUVECs monolayers were infected at an m.o.i. of 25 pfu/cell with either a control GFP-encoding AV or AV/myc-human A_{2A}AR. After treatment with or without 10 ng/ml TNF α for the indicated times, soluble cell extracts were prepared and equalised for protein content prior to SDS-PAGE and immunoblotting with anti-I κ B α antibody. This is one of multiple experiments.

Panel C: HUVECs plated onto glass coverslips were infected at an m.o.i. of 25 pfu/cell with either control AV/GFP or GFP AV/myc-human A_{2A}AR, which also expresses GFP from a separate open reading frame. After treatment with or without 10 ng/ml TNF α for 60 min as indicated, cells were fixed, permeabilised and p65 identified by staining with a p65-specific antibody and Alexa594-conjugated anti-rabbit IgG and dual label confocal microscopy as described in the Materials and Methods. HUVECs expressing recombinant protein are visible as *green* from GFP-derived fluorescence, while endogenous p65 is visible as *red*. This is one of multiple experiments.

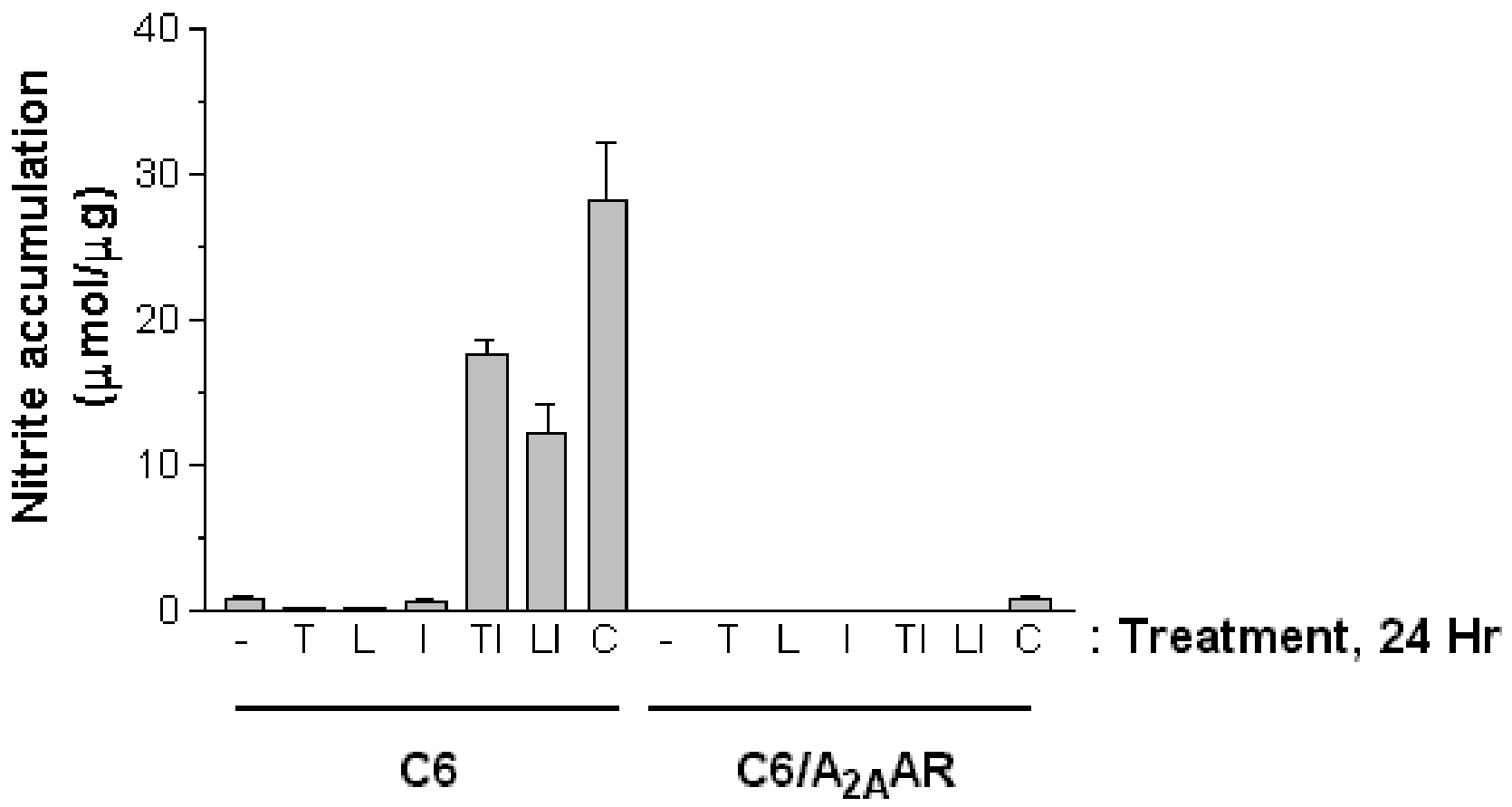


Figure 1A

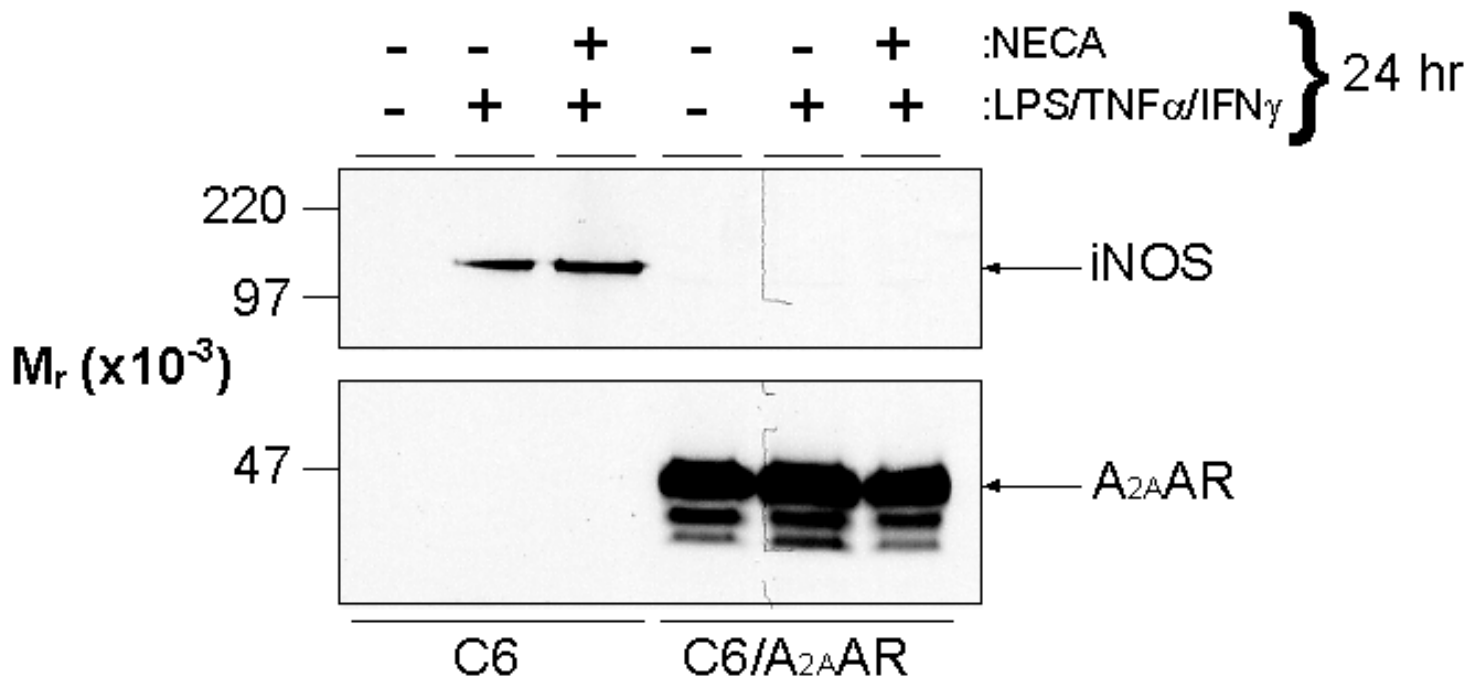


Figure 1B

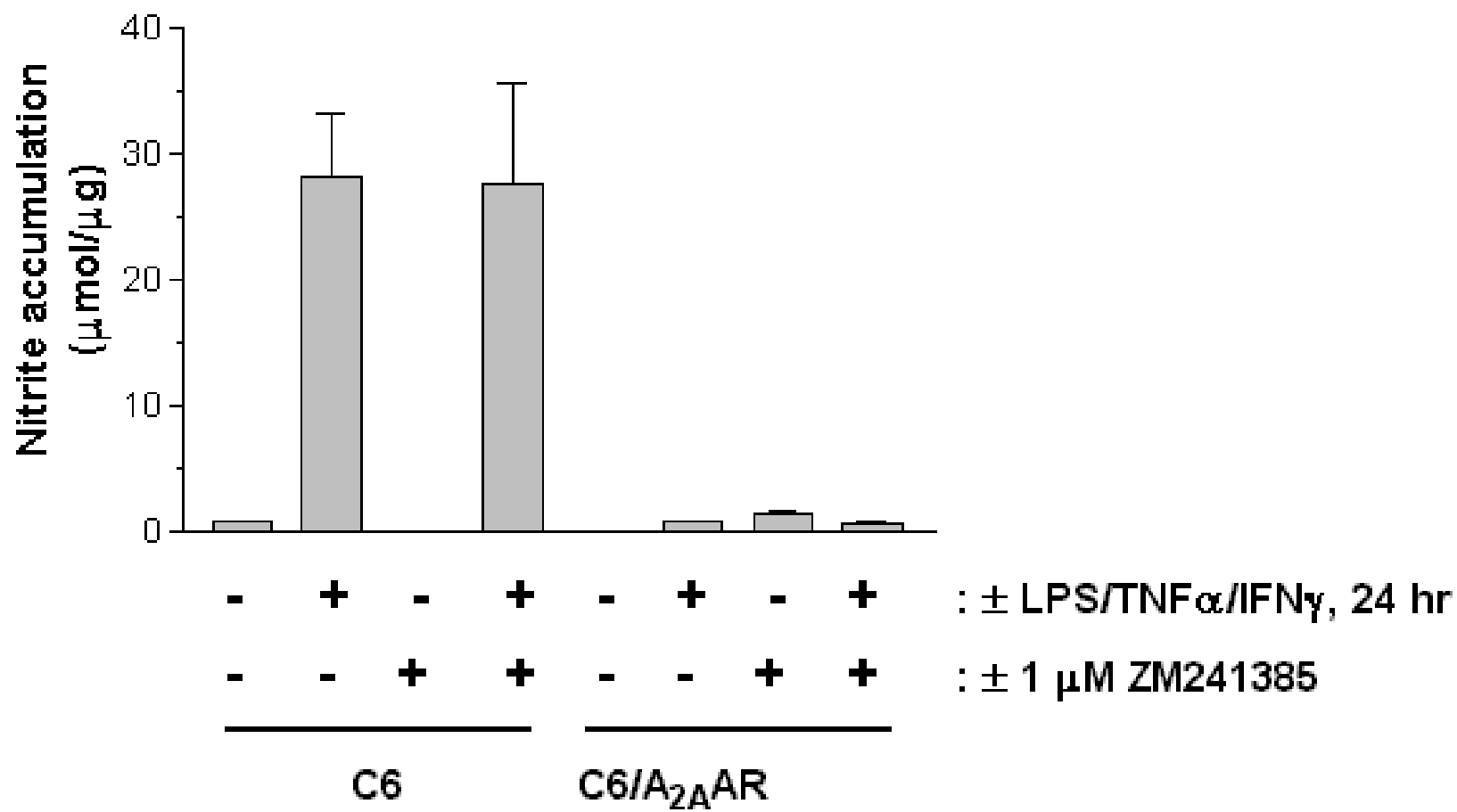


Figure 1C

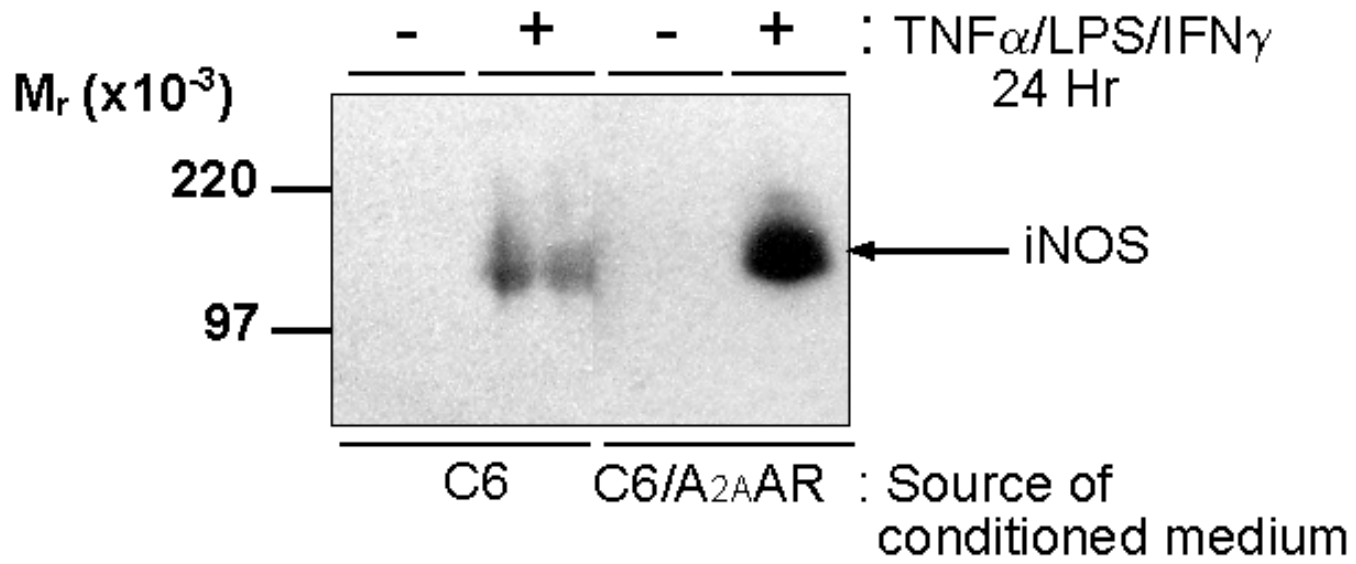


Figure 2

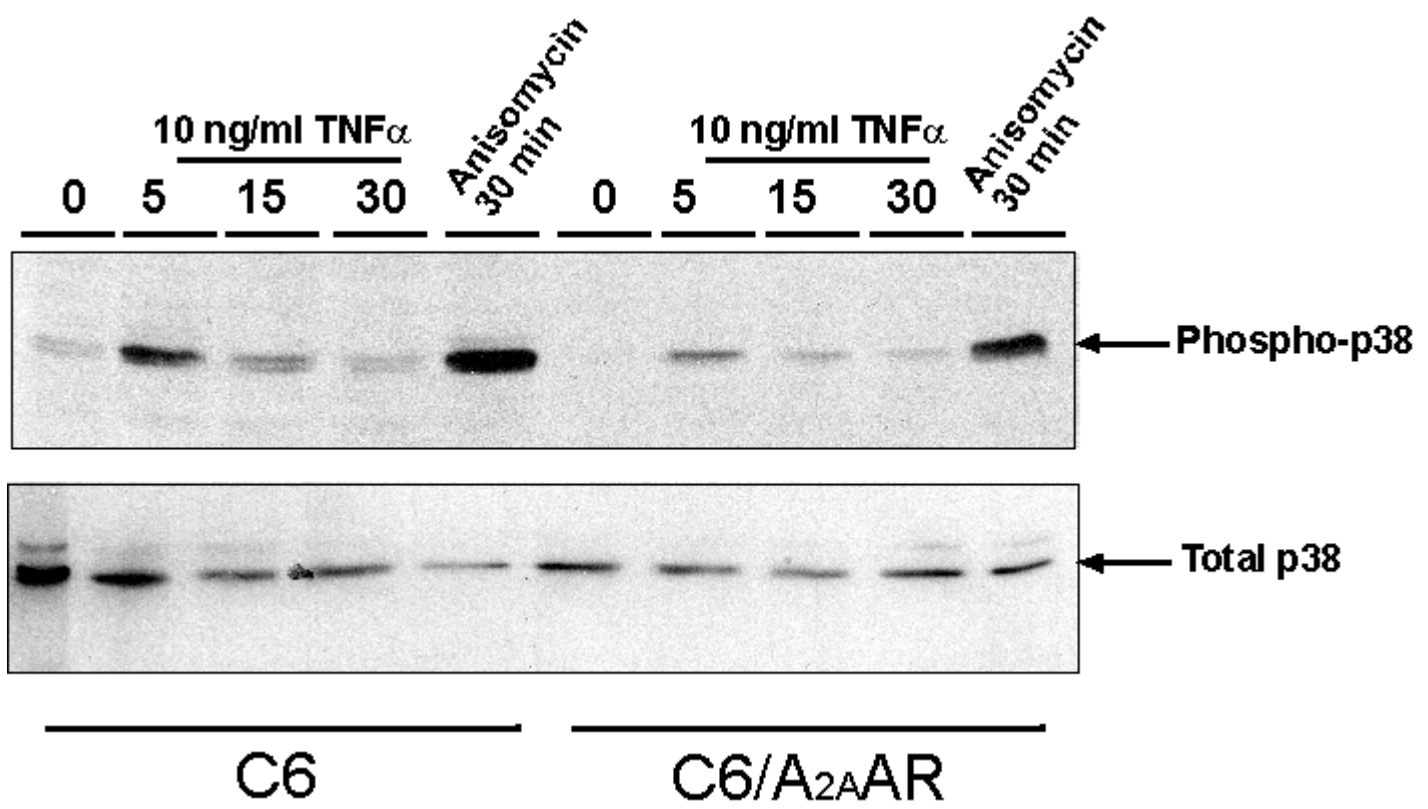


Figure 3A

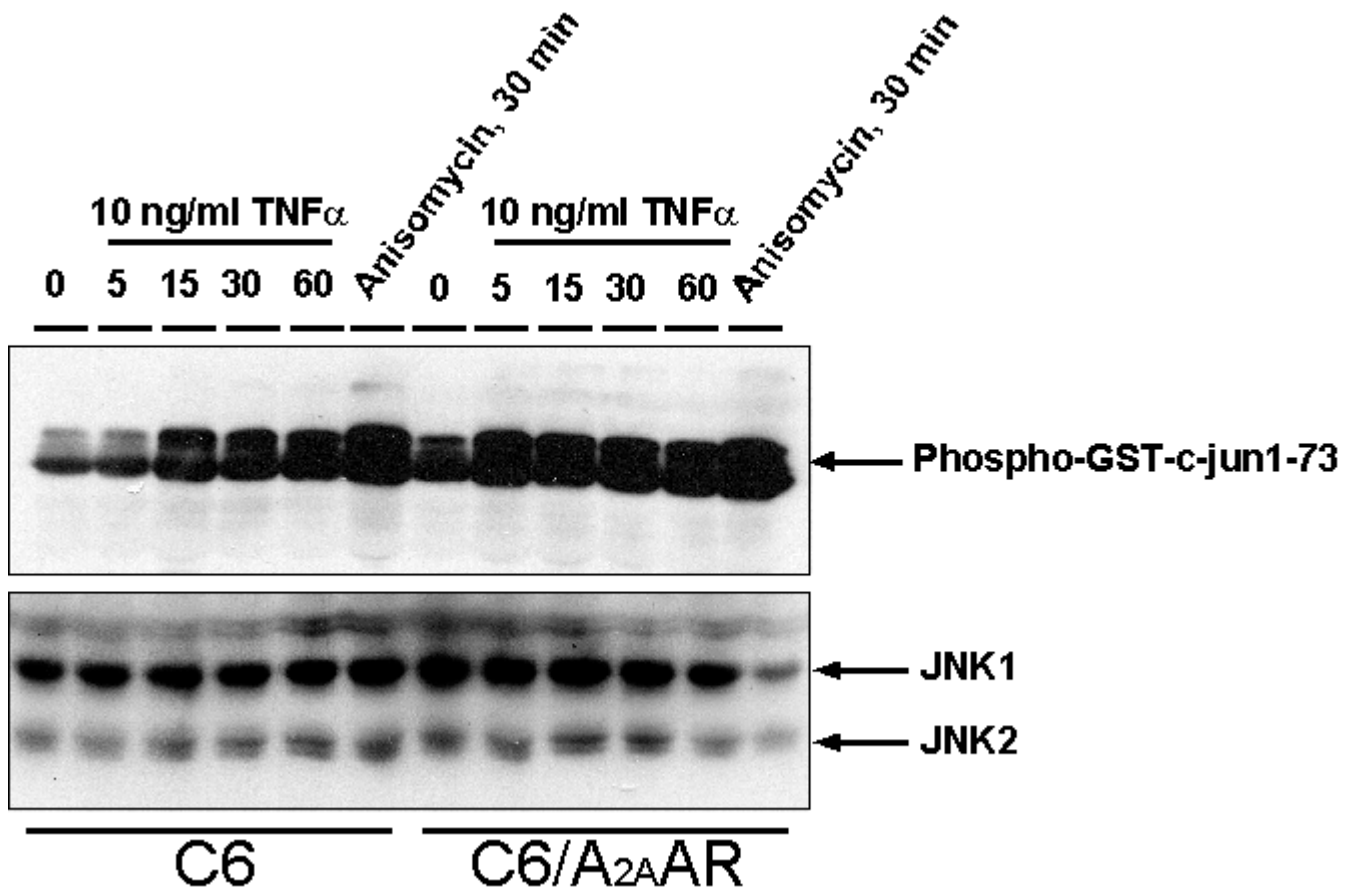


Figure 3B

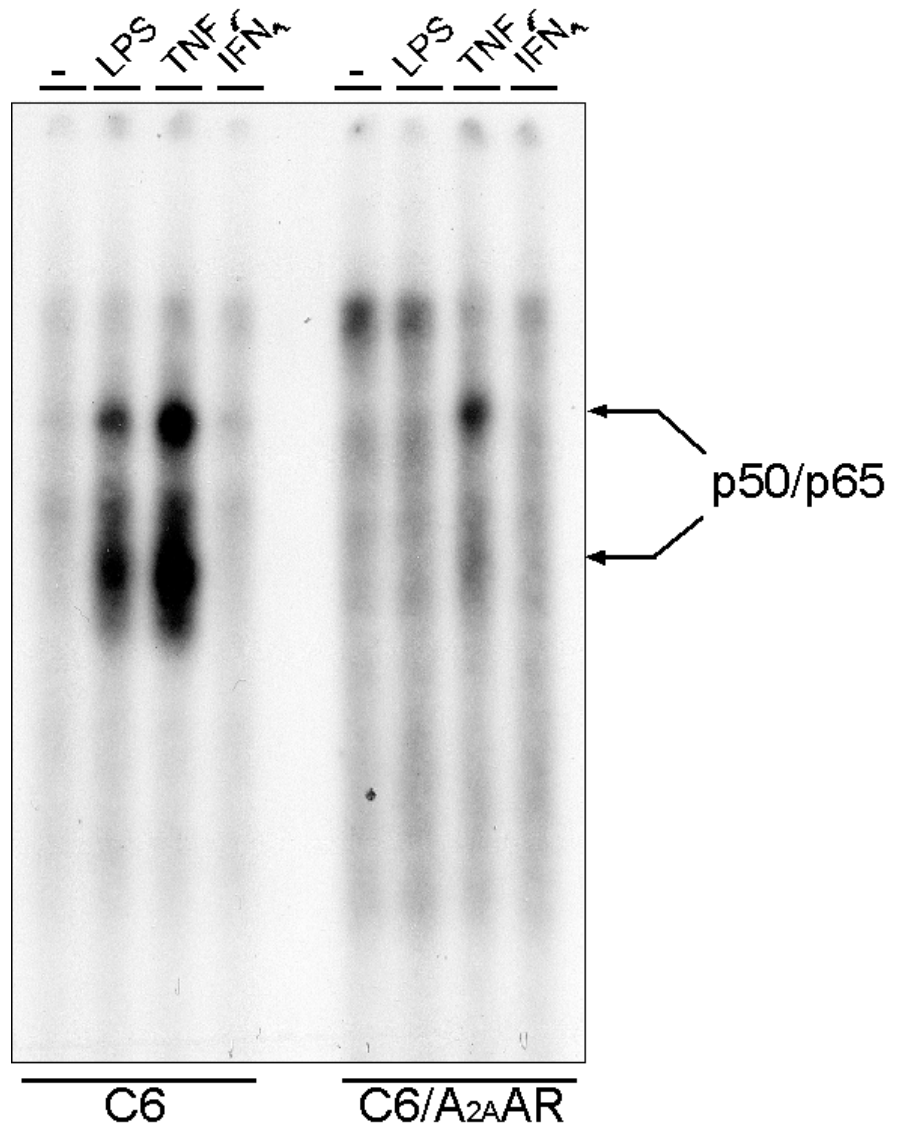


Figure 4A

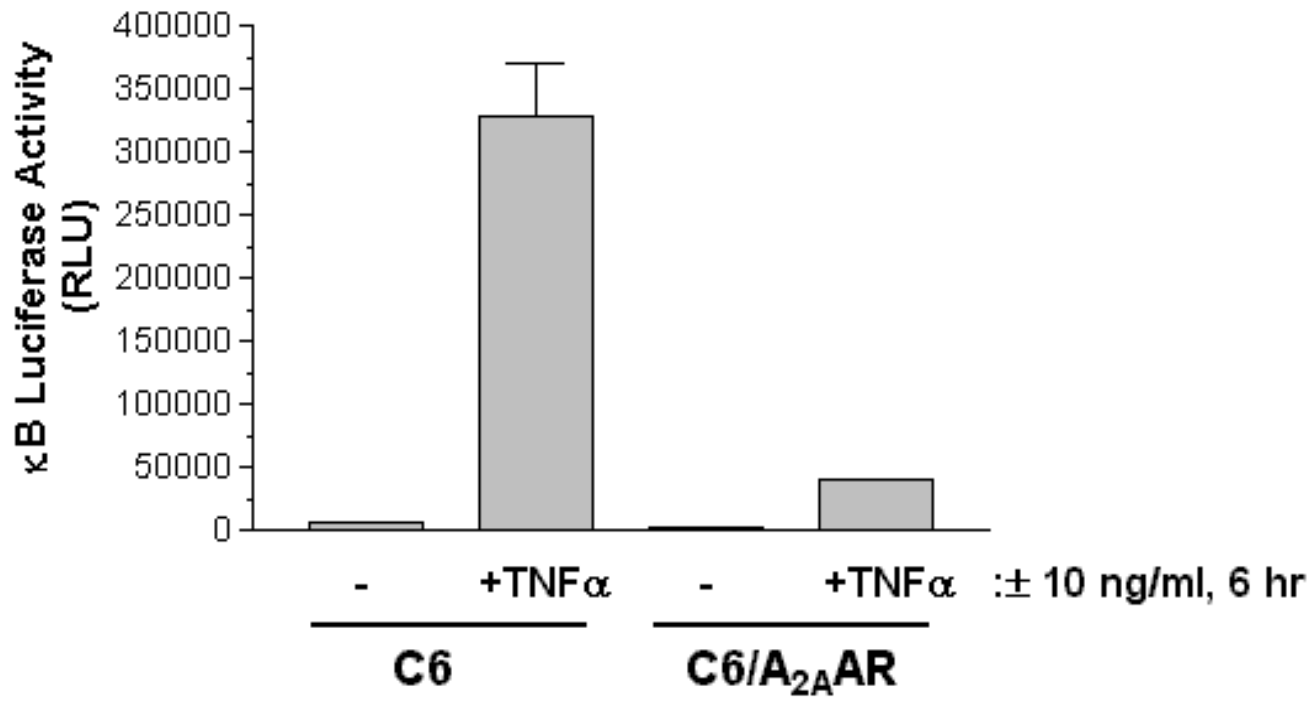


Figure 4B

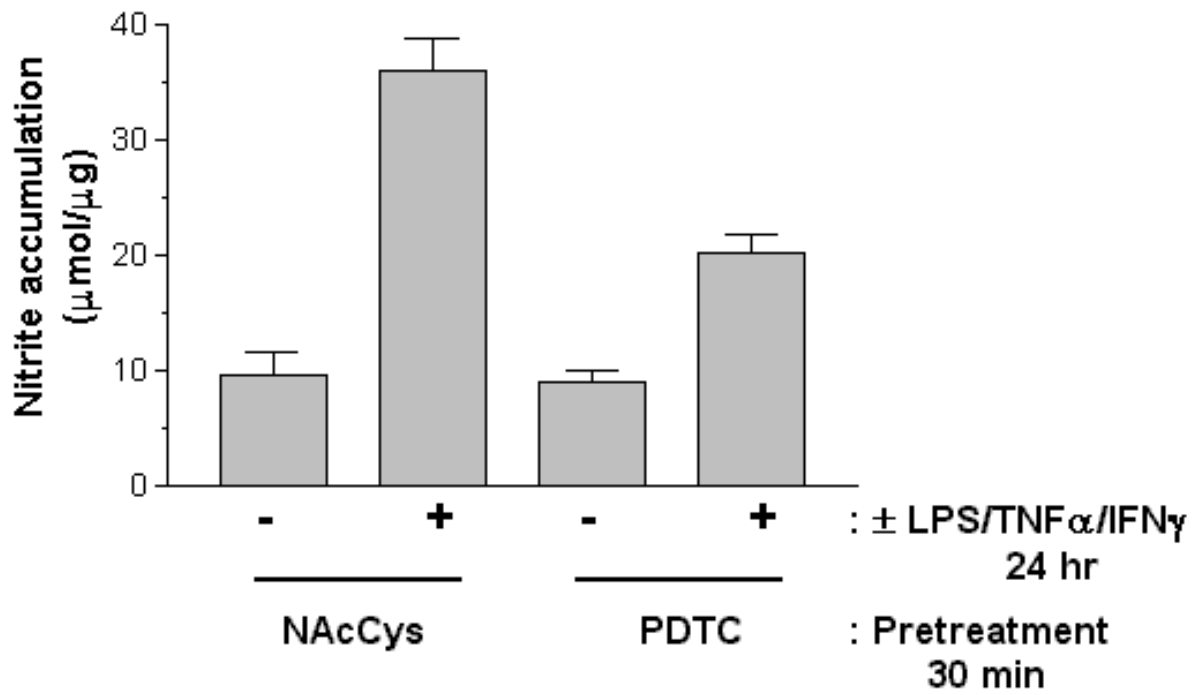


Figure 5A

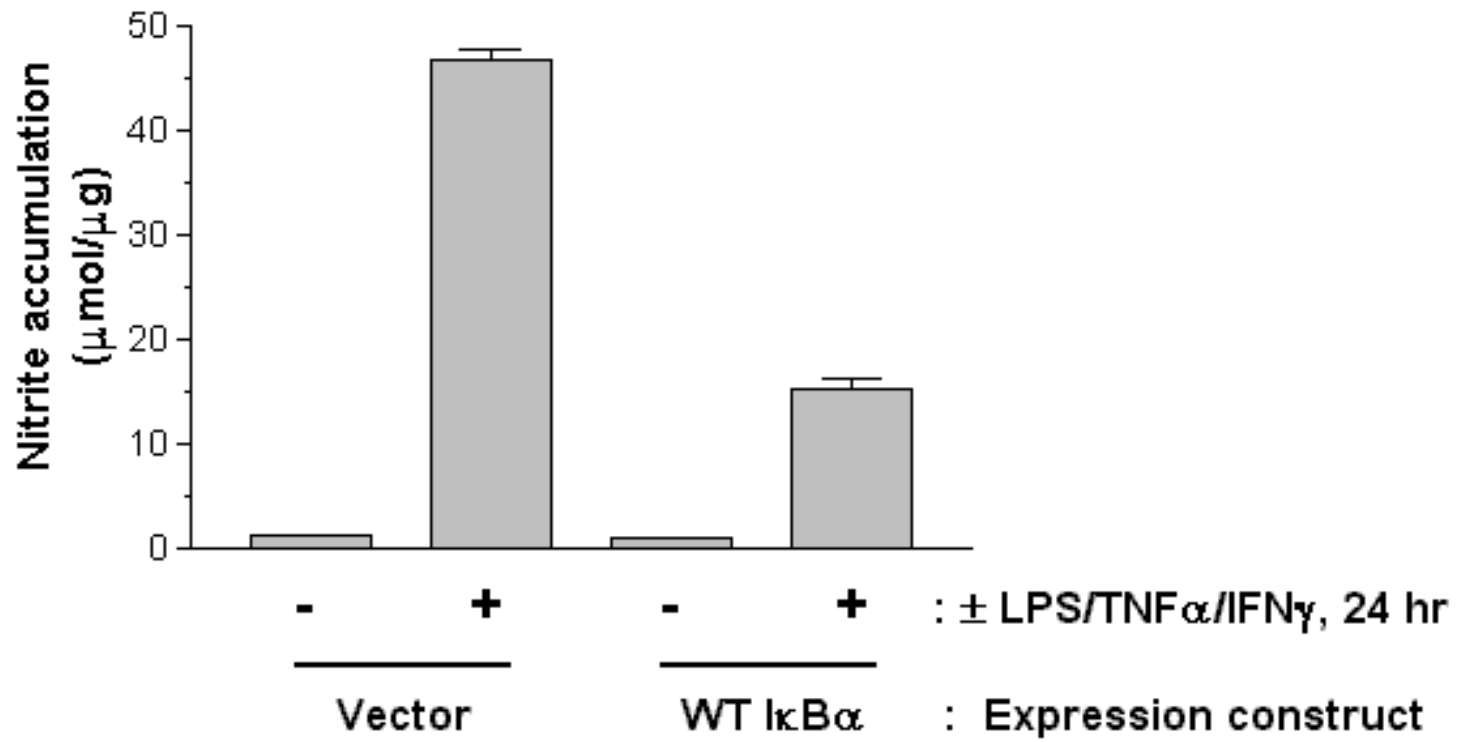


Figure 5B

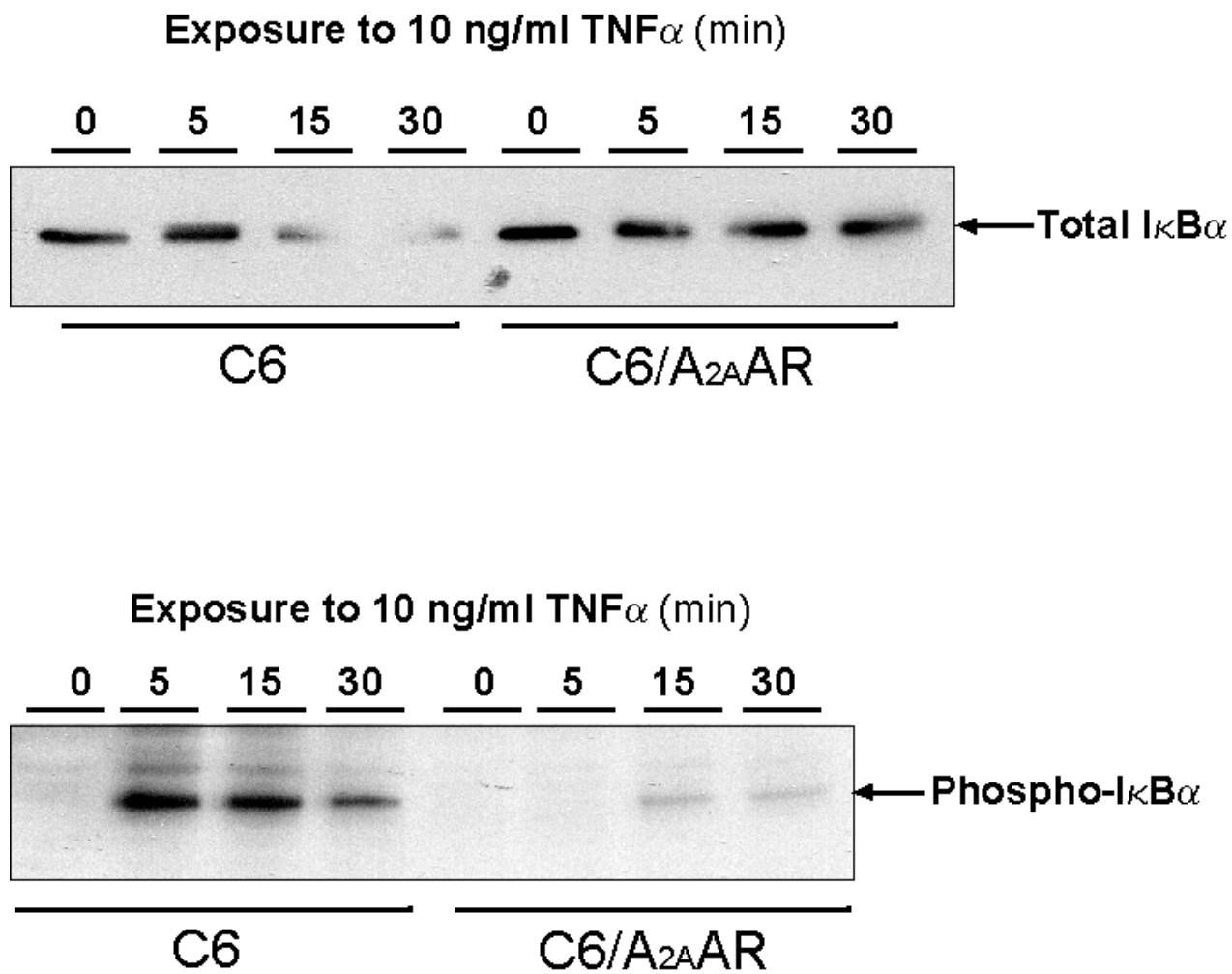


Figure 6A

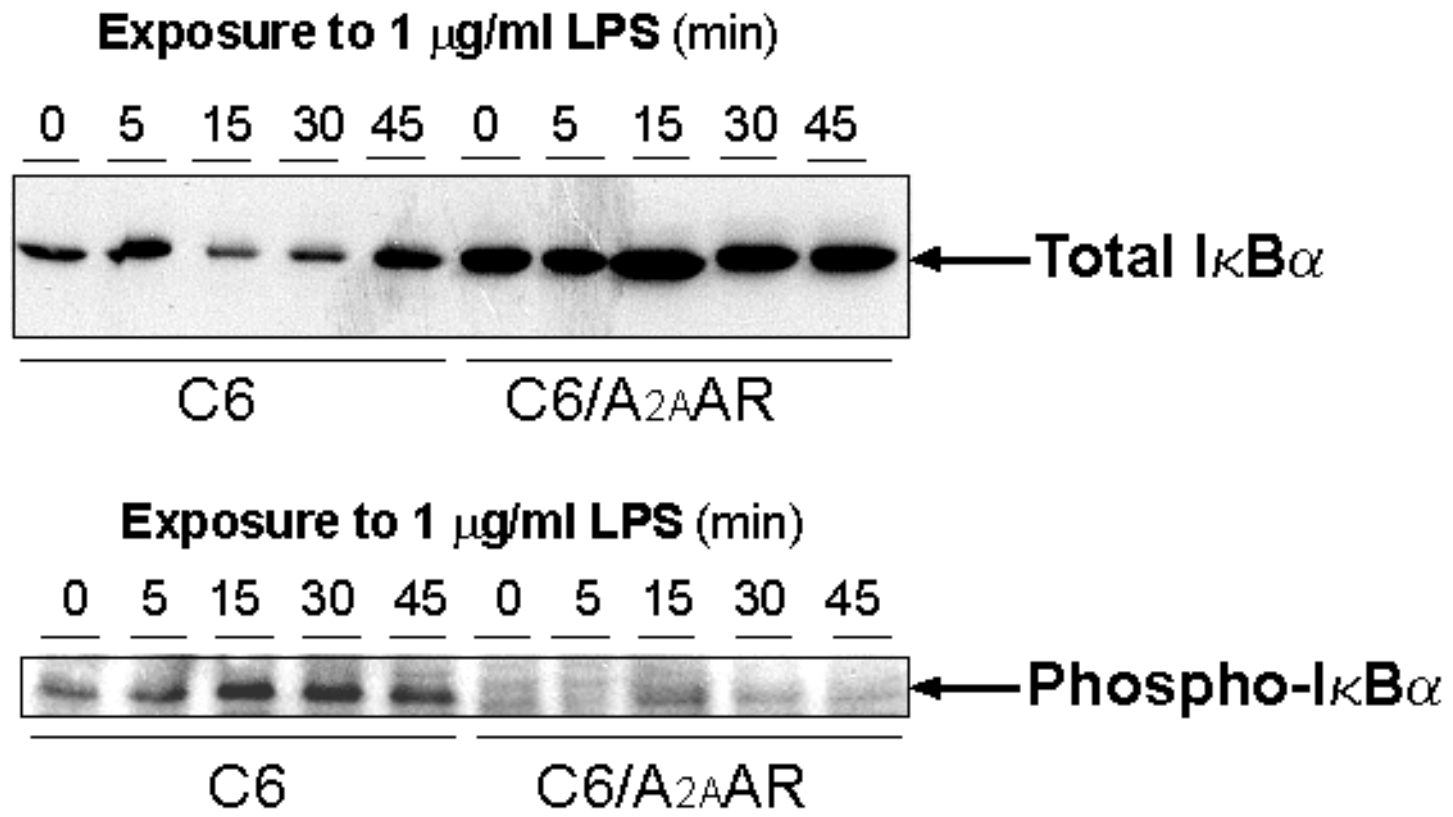


Figure 6B

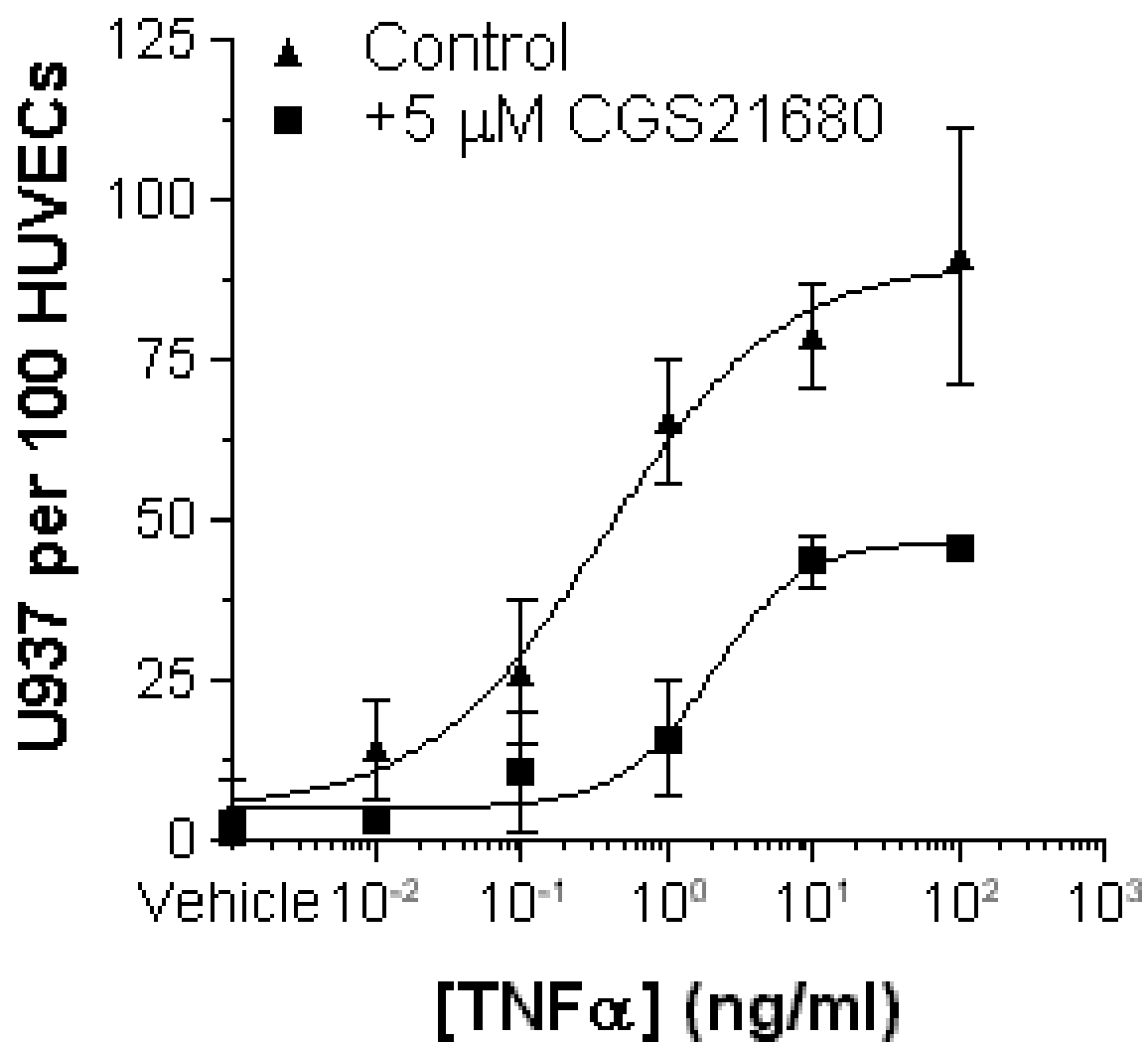


Figure 7A

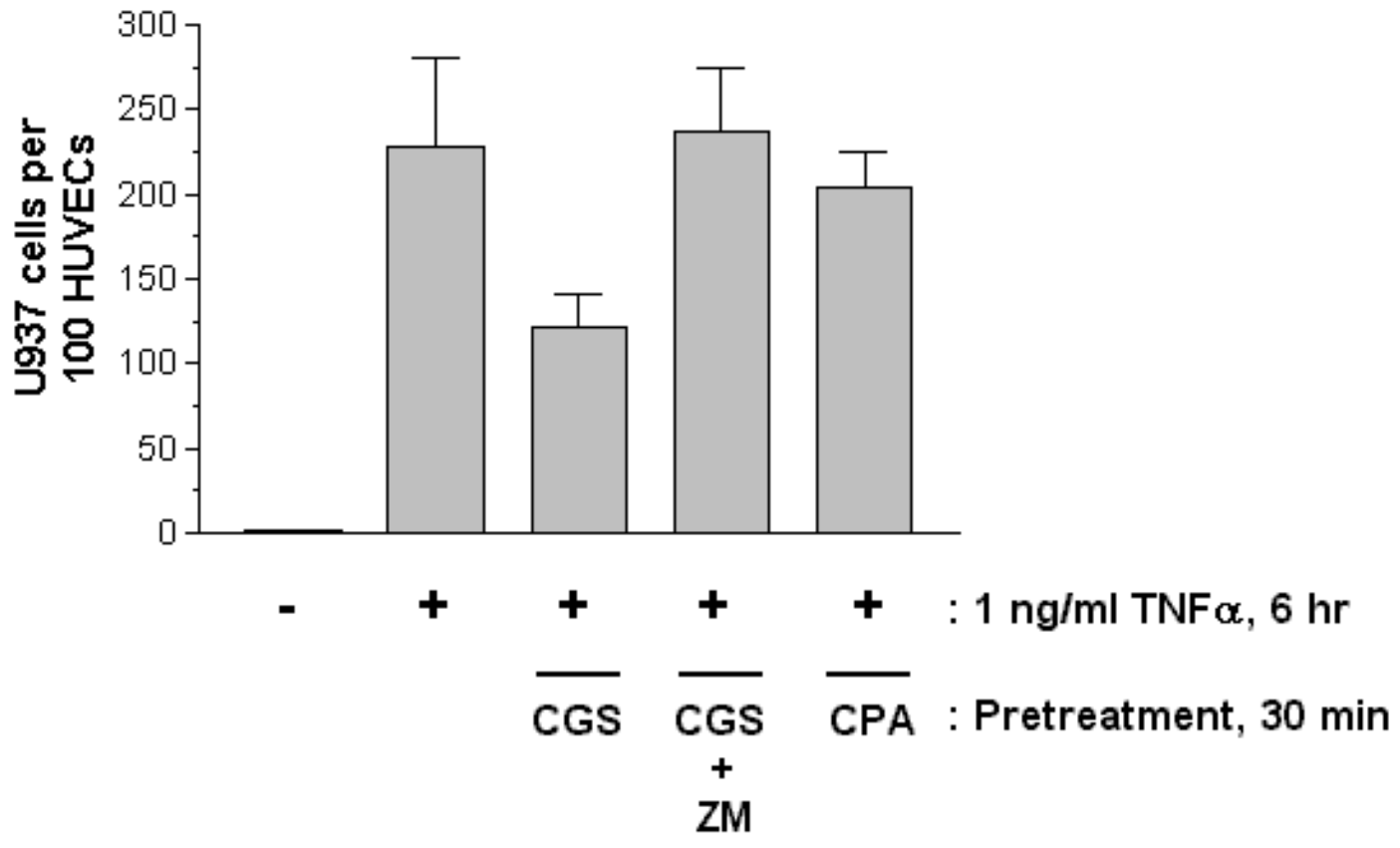


Figure 7B

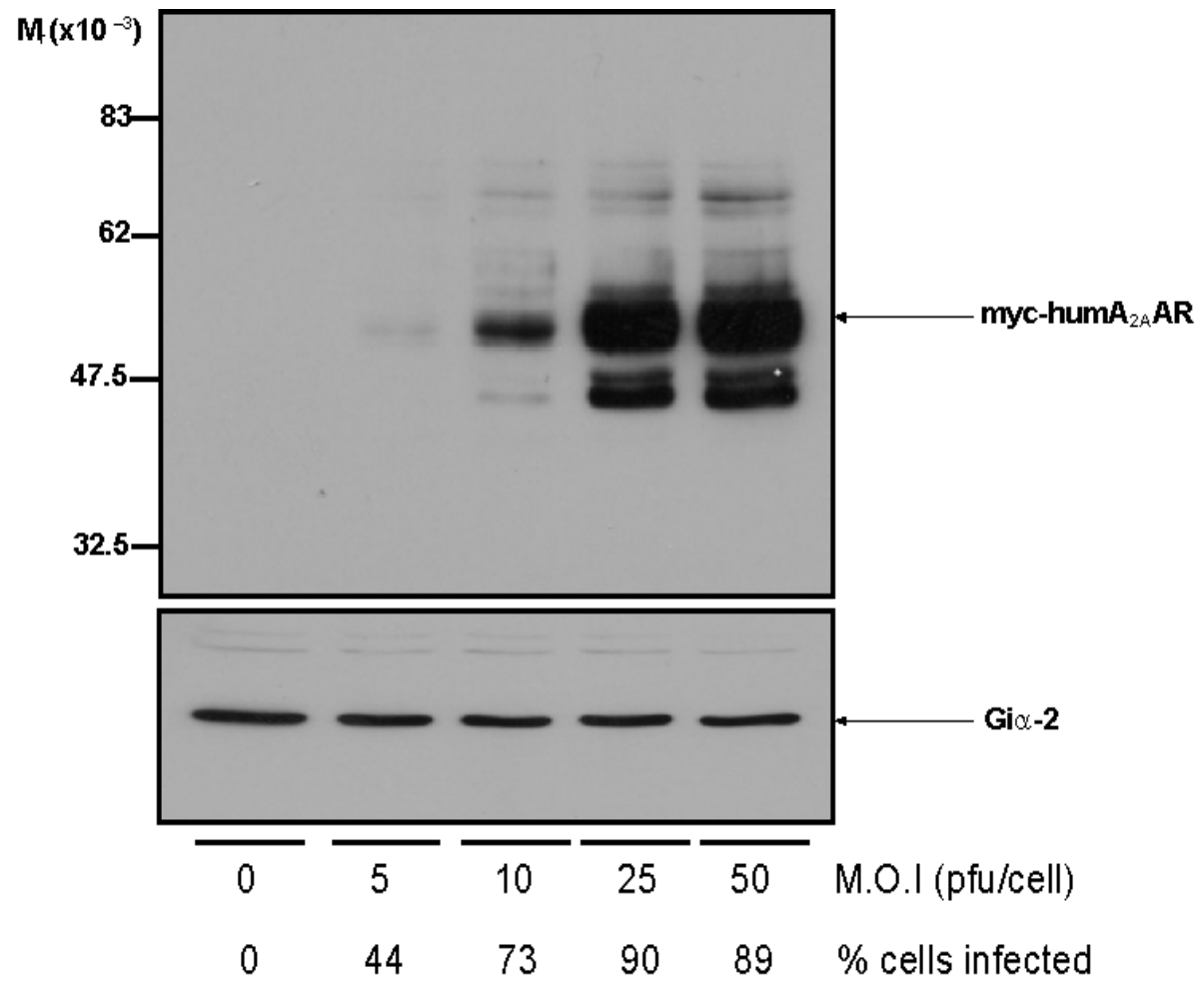


Figure 8A

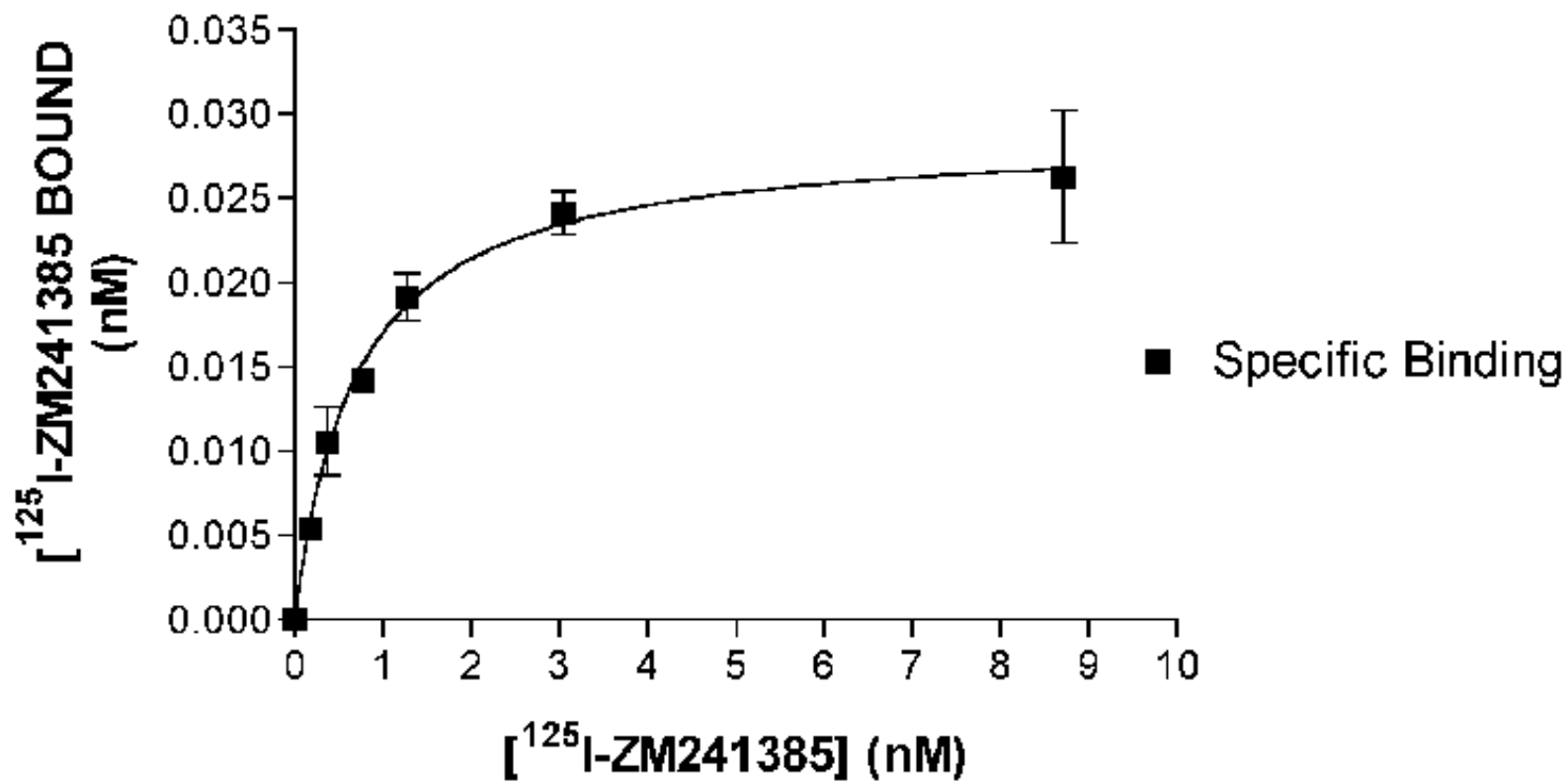


Figure 8B

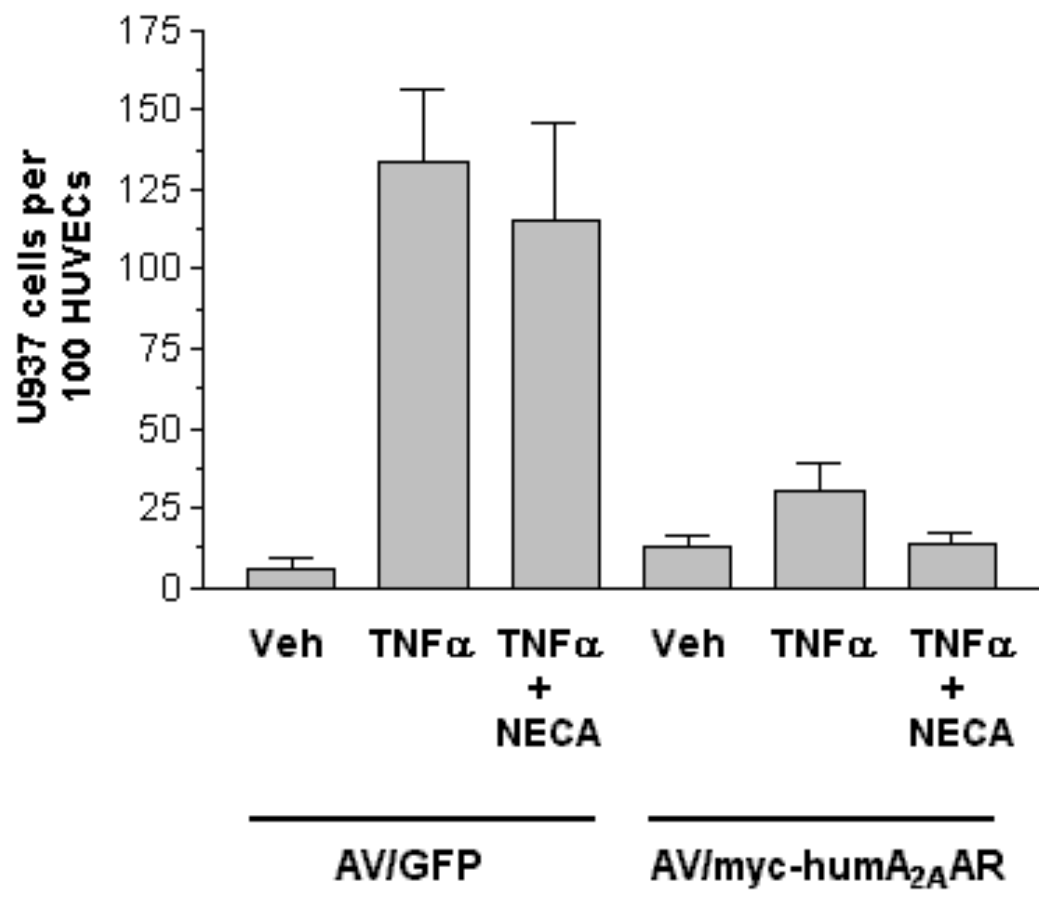


Figure 9

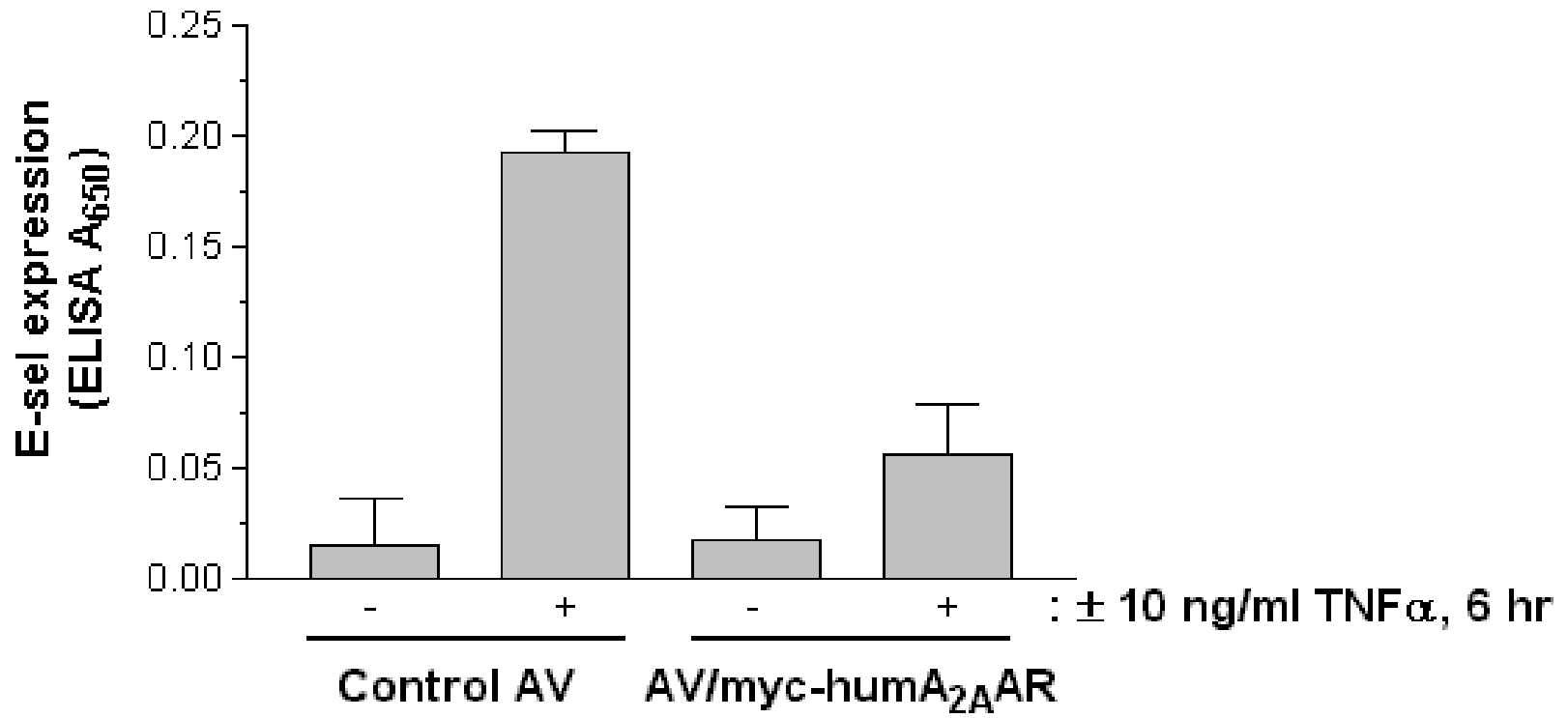


Figure 10A

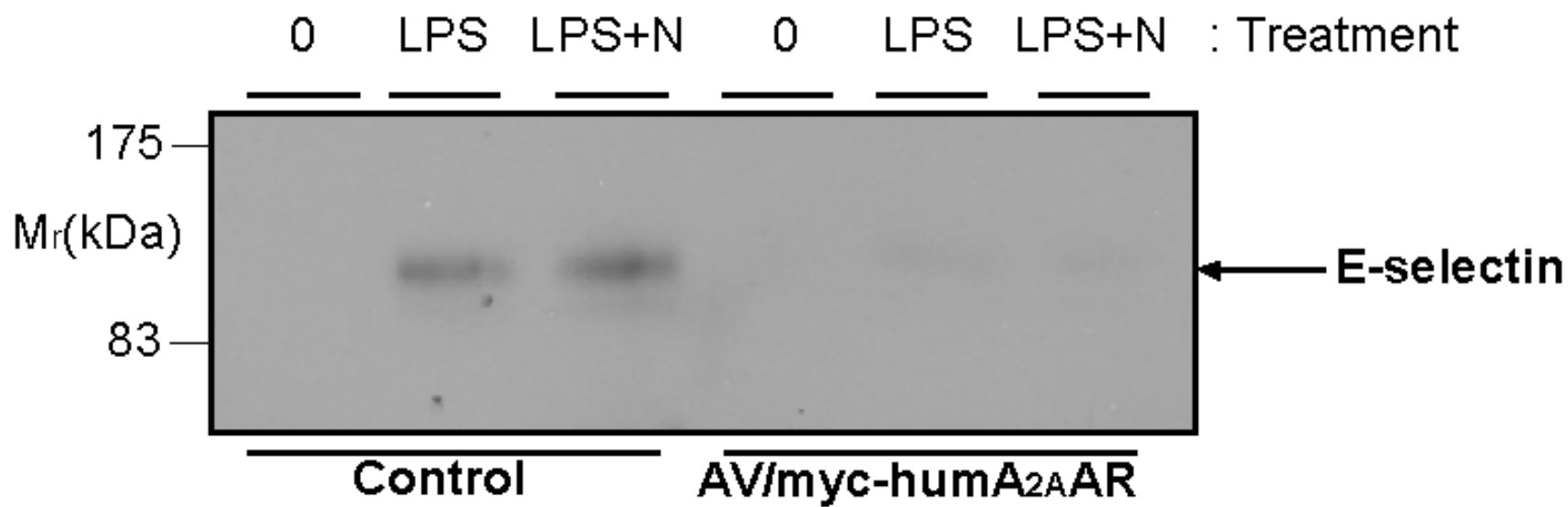


Figure 10B

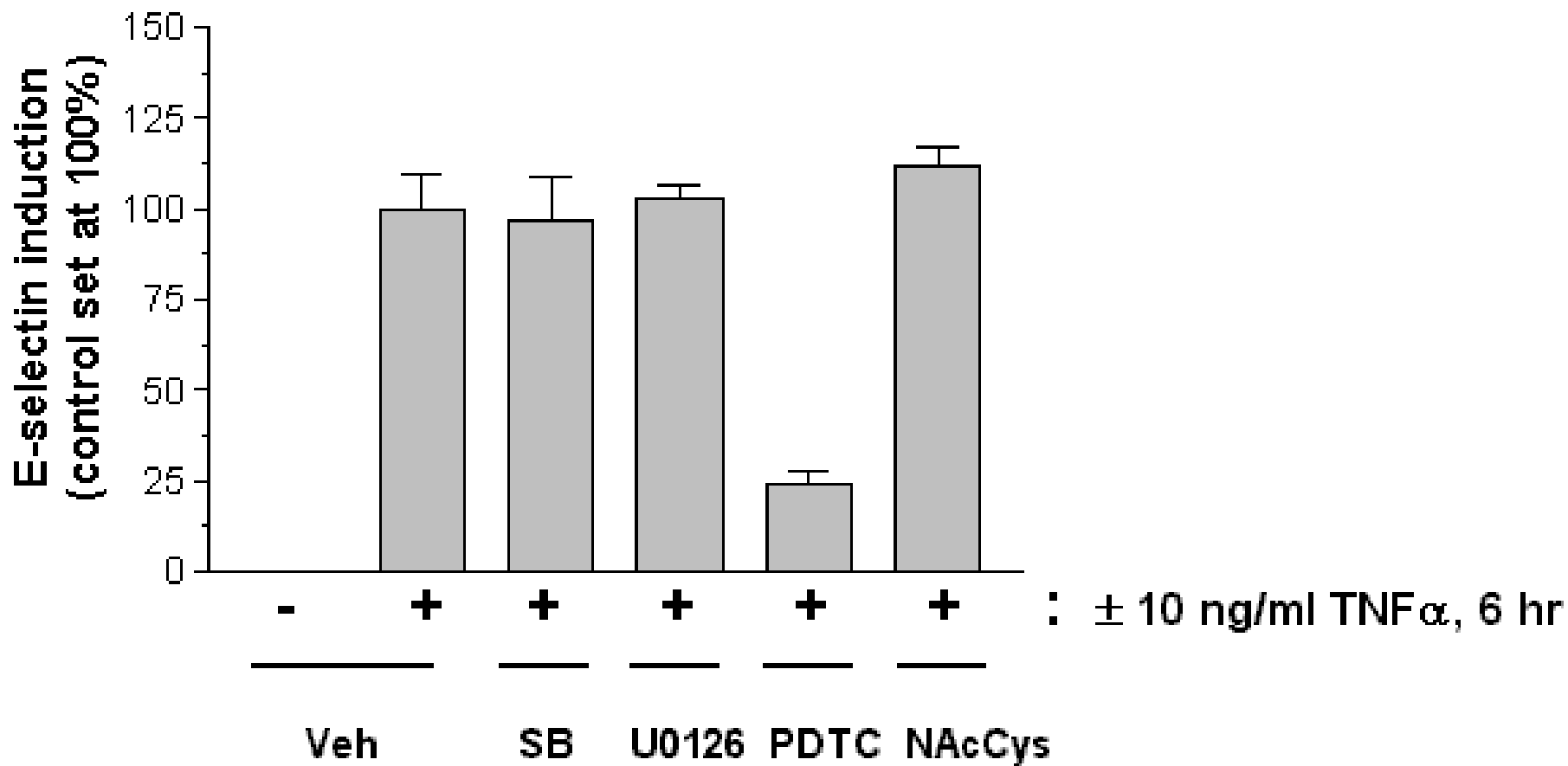


Figure 11A

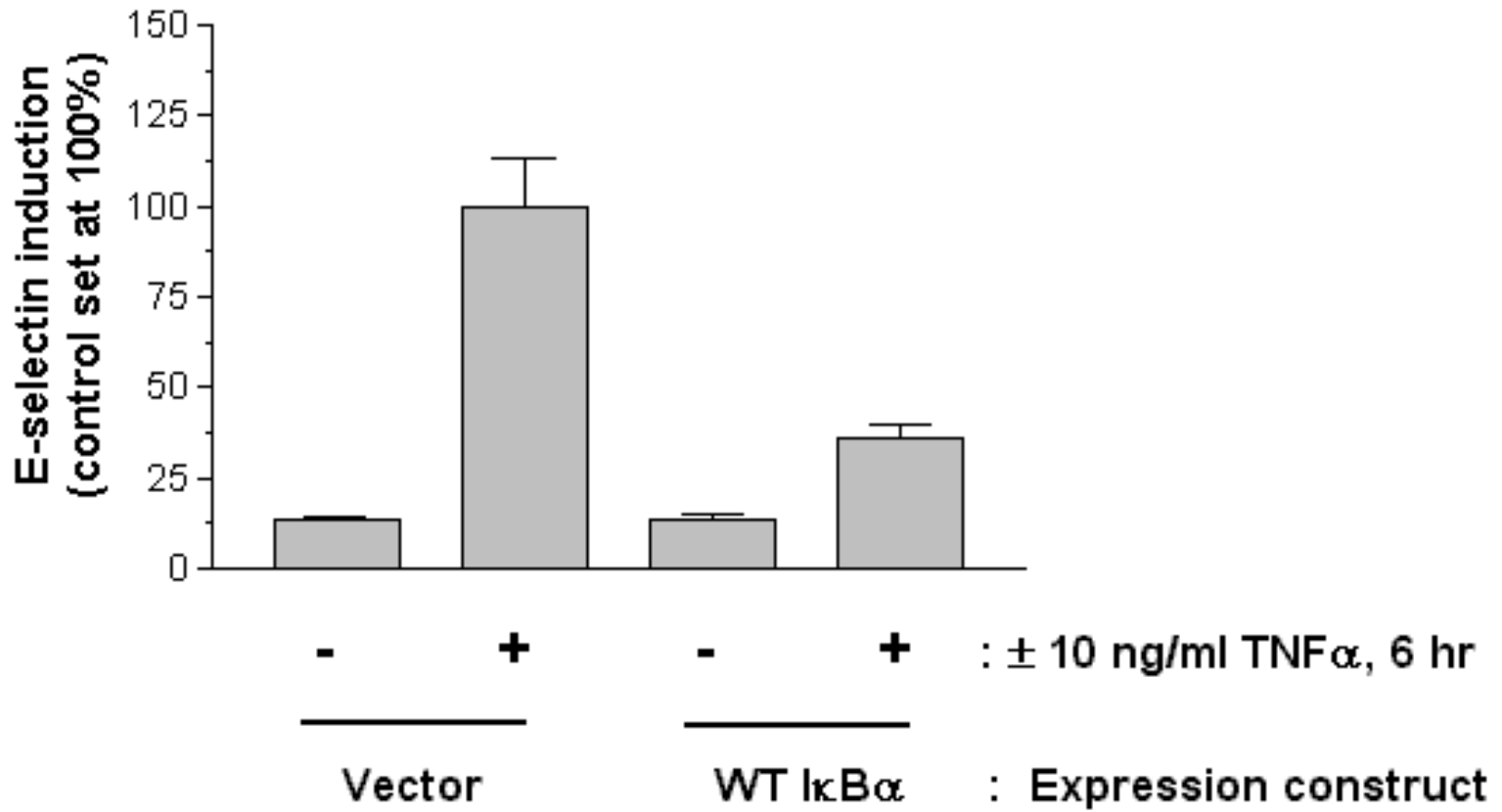


Figure 11B

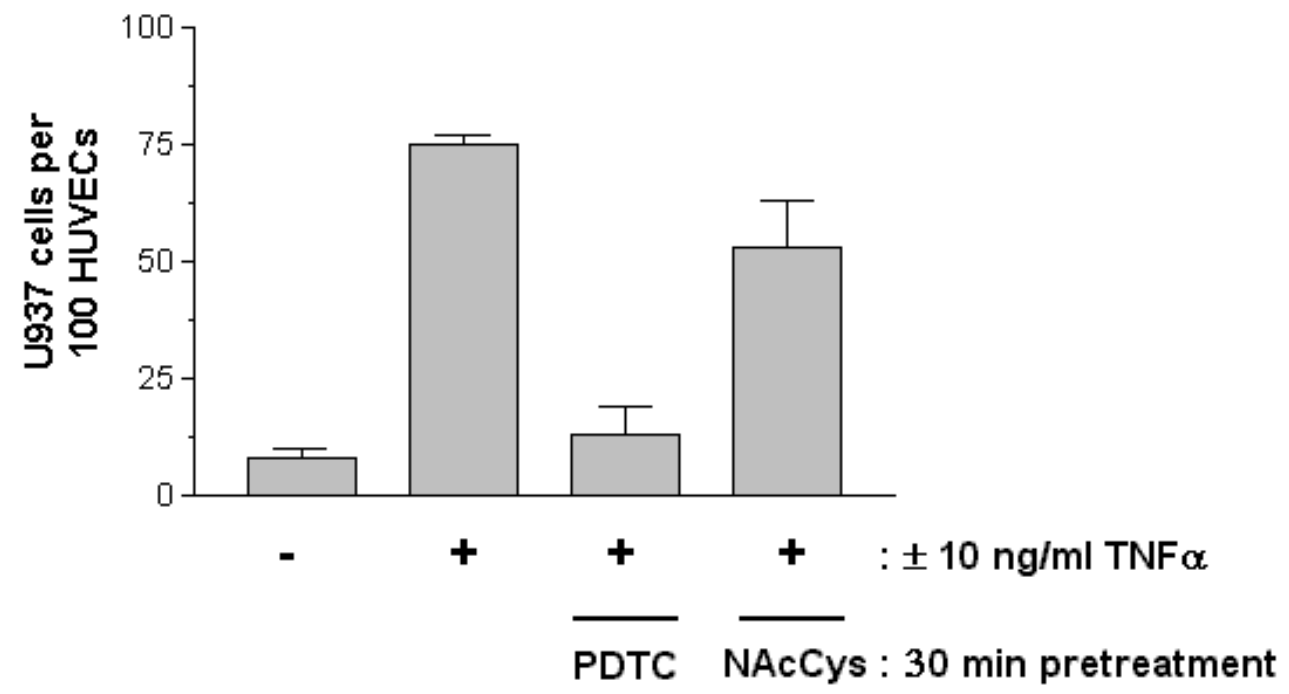


Figure 11C

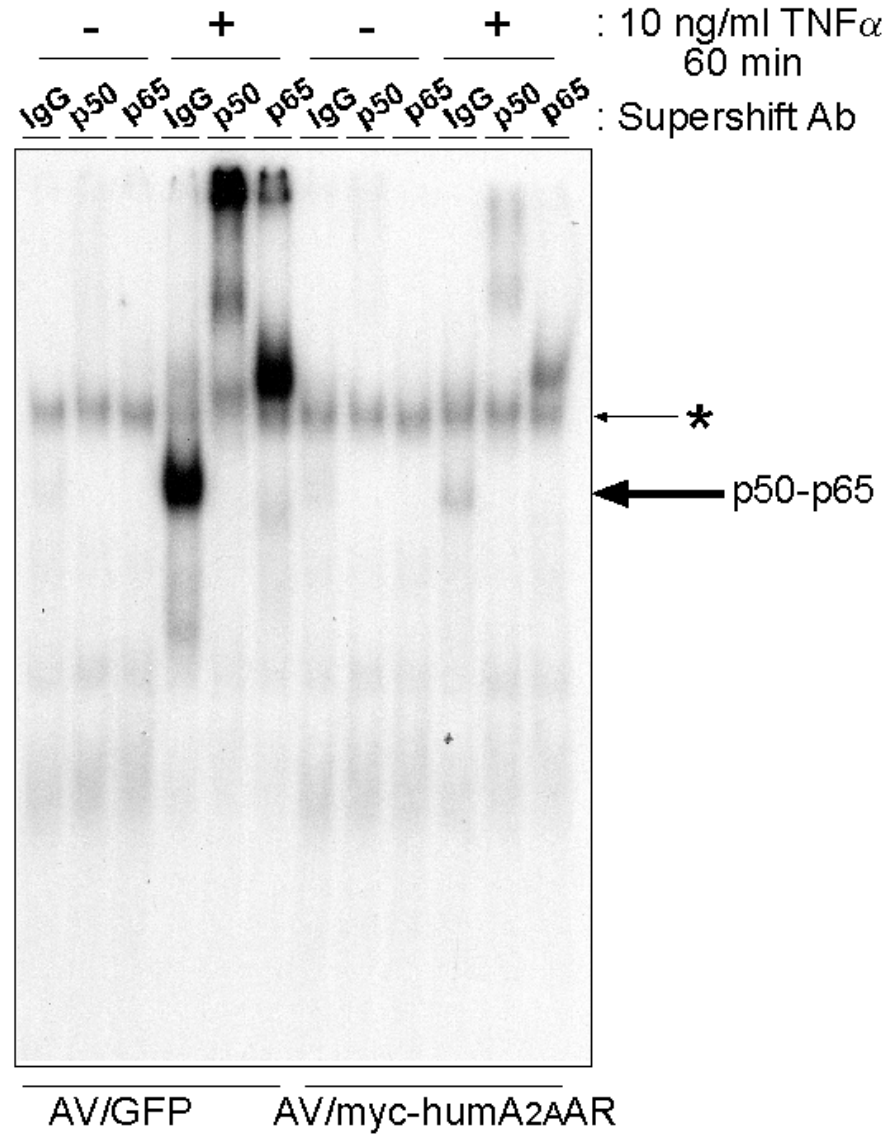


Figure 12A

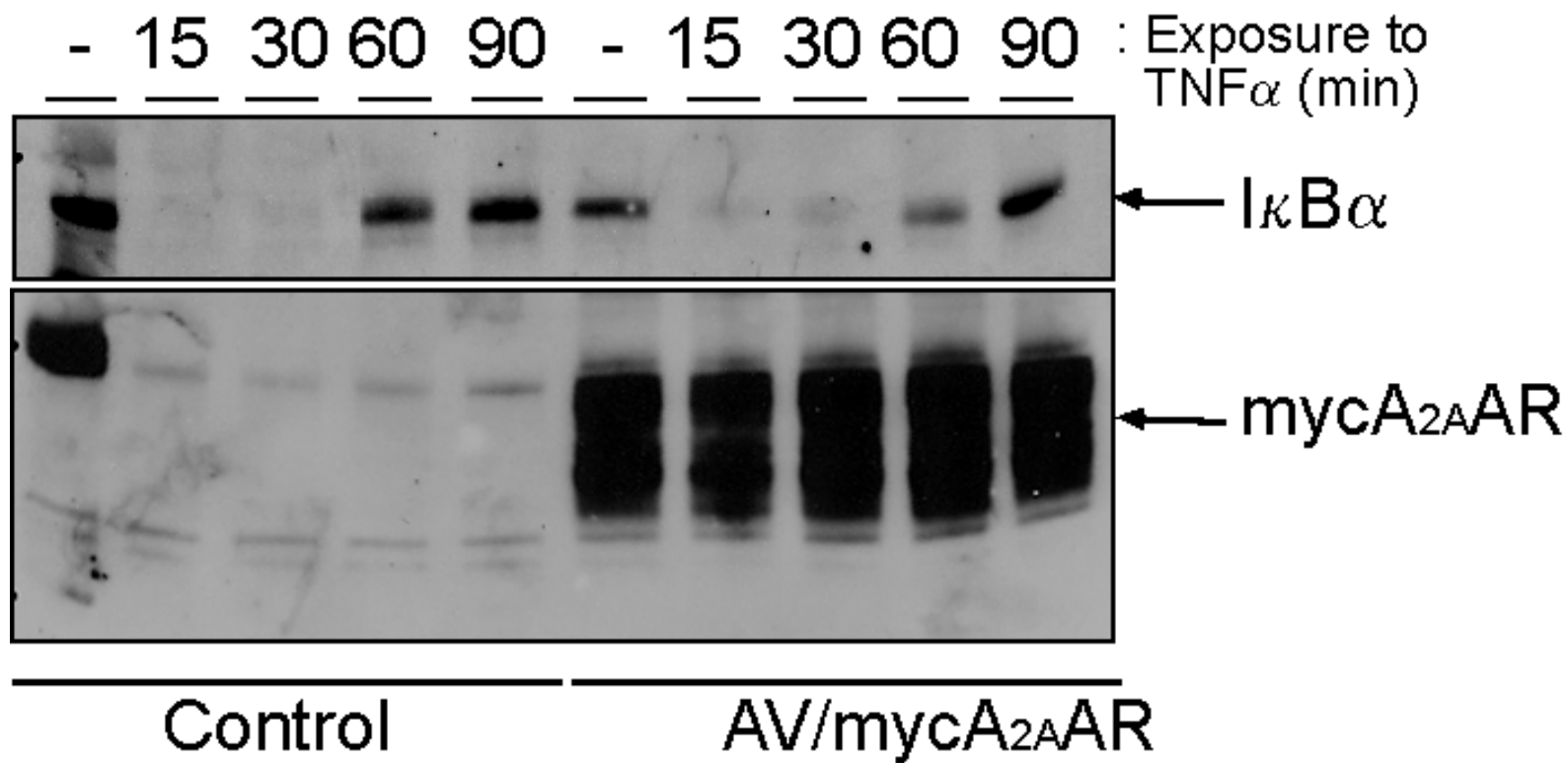


Figure 12B

AV-GFP

AV/myc-humA_{2A}AR

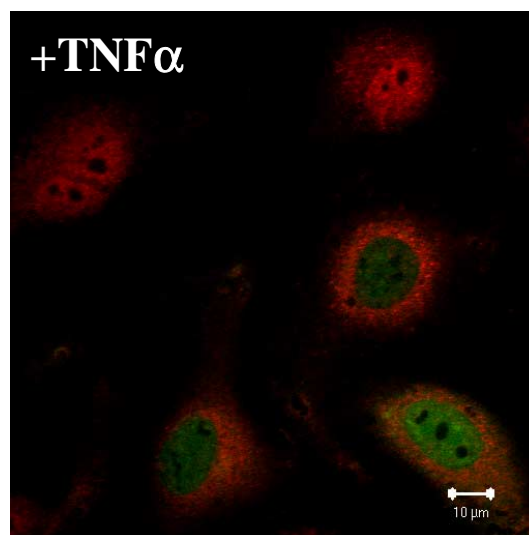
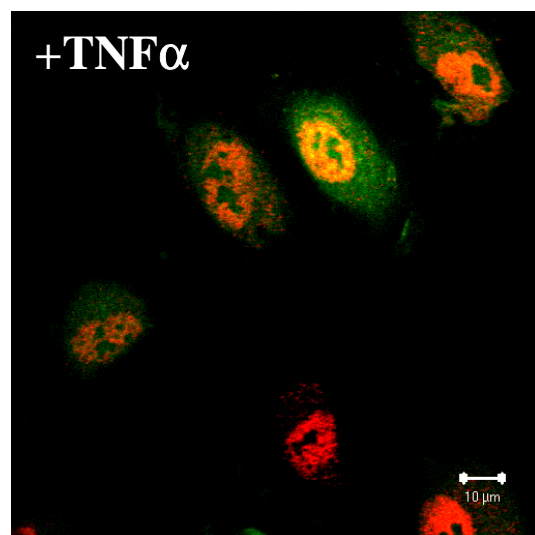
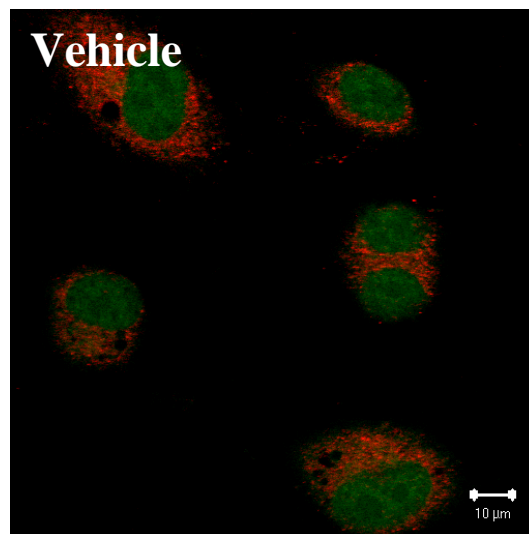
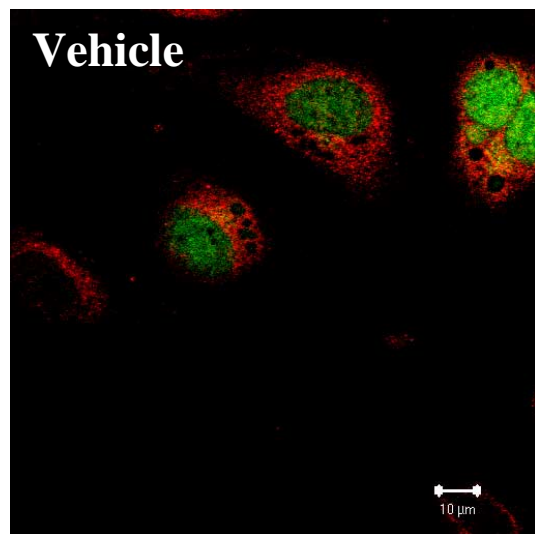


Figure 12C